社團法人中華鋪面工程學會
Chinese Society of Pavement Engineering

ORIGINAL RESEARCH PAPER

Improvement of Low Plasticity Clay with Crushed Glass: A Mechanical and Microstructural Study

Salpadoru Tholkamudalige Anupiya M. Perera[1] · Mohammad Saberian[1] · Jiasheng Zhu[1] · Rajeev Roychand[1] · Jie Li[1] · Gang Ren[1] · Morteza Tahmasebi Yamchelou[1]

Abstract

Low plasticity clays are found in abundance worldwide, exerting undue stresses on civil structures, road pavements and railway infrastructure, owing to the periodic settlement caused by their low bearing capacity and slight swelling potential. They are often encountered as natural soil when constructing road subgrade and have the potential to compromise the integrity of the entire pavement system unless improved appropriately. Furthermore, the accumulation of vast quantities of non-biodegradable glass waste is identified as a challenge in many countries. Considering the above, this paper aims to provide a sustainable solution by studying the effect of crushed glass (CG) at varied inclusions of 0, 5, 10, 15 and 20% in a clay subgrade. The testing procedure implemented includes three distinct testing phases, namely, material properties, microstructural properties and mechanical strength tests. The material property tests involved particle size distribution, X-ray fluorescence (XRF) and X-ray diffraction (XRD) testing. Microstructural tests considered include scanning electron microscope (SEM) and micro-CT (CT) testing, which enabled a vital understanding of how the introduction of glass affects the internal structure of the clay matrix, where an increase in the porosity was evident upon adding CG. The mechanical testing phase involved standard compaction, unconfined comprehensive strength (UCS), California bearing ratio (CBR), resilient modulus and swelling–shrinkage tests. It can be concluded that introducing CG improved the clay's mechanical strength with respect to UCS, CBR and resilient modulus whilst also reducing its swelling potential, where the optimum inclusion of CG at 15% best enhanced the mechanical strength properties of the low plasticity clay.

Keywords Low plasticity clay · Crushed glass · Soil improvement · Pavement subgrade

Salpadoru Tholkamudalige Anupiya M. Perera and Mohammad Saberian are joint first authors.

✉ Mohammad Saberian
mohammad.boroujeni@rmit.edu.au

Salpadoru Tholkamudalige Anupiya M. Perera
salpadoru.perera@rmit.edu.au

Jiasheng Zhu
s3557884@student.rmit.edu.au

Rajeev Roychand
rajeev.roychand@rmit.edu.au

Jie Li
jie.li@rmit.edu.au

Gang Ren
gang.ren@rmit.edu.au

Morteza Tahmasebi Yamchelou
Morteza.TahmasebiYamchelou@roads.vic.gov.au

[1] School of Engineering, RMIT University, Melbourne, VIC, Australia

Abbreviations

CG	Crushed glass
MDD	Maximum dry density
OMC	Optimum moisture content
UCS	Unconfined compressive strength
CBR	California bearing ratio
XRF	X-ray fluorescence
LL	Liquid limit
RLT	Repeated load triaxial
M_r	Resilient modulus
SEM	Scanning electron microscope
X-ray MicroCT	X-ray microcomputed tomography
XRD	X-ray diffraction

∯ Springer

1 Introduction

Road networks are an integral component of infrastructure, enabling travel and paving the path for commerce, thereby directly influencing the advancement of the economy and the standard of living of a country [1]. The subgrade layer of roads is generally made of untreated natural soil; however, certain types of soil, including expansive clays, have poor mechanical qualities, namely low strength, high compressibility and swelling–shrinkage properties [2–5]. The aforementioned properties adversely affect the stability of buildings, lightweight structures and infrastructure around the globe [6–11], adding to the financial burden on governments and eventually the taxpayers. Swell–shrink soils are commonly encountered during the construction of roads and infrastructure, often leading to complications during construction as well as negatively affecting the longevity of the pavement as a result of the undesirable attributes mentioned afore. In projects undertaken in the past, inferior naturally occurring soils were excavated and replaced entirely with higher quality aggregates [12, 13]. However, the scarcity of road materials has now led to an increased interest in the improvement of existing natural soils for use as road subgrade as opposed to their replacement [14]. There are two major categories of soil improvement, mechanical and chemical improvement. The mechanical improvement involves the addition of supplementary materials consisting of mechanical and physical properties (such as hydrophobicity) that are in contrast to the properties of the clay. The addition of such materials aid in alleviating the undesirable qualities of the natural clay [15–21]. Chemical improvement, on the other hand, utilises binders that enable chemical reactions that aid in consolidating the clay. These binders may be introduced in various forms, including cement, slake lime (calcium hydroxide), fly ash, polymers, resins, zeolite, enzymes, etc. [22–28]. Although chemical improvement is found to be effective, a majority of traditional chemical stabilisers are identified as significant contributors to the build-up of greenhouse gases in addition to having high costs of production [29–32]. The recent decades have brought about remarkable changes in the engineering sector, where an approach with sustainability as a focal point has been widely adopted, resulting in mechanical improvement becoming the preferred form of soil improvement. Furthermore, governments encourage the utilisation of waste materials wherever feasible in construction projects, thereby helping to conserve natural quarried aggregate whilst also providing a beneficial use for stockpiled waste. Some of those recycled waste materials that have been used for road construction are reclaimed construction and demolition waste [33–36] and crushed glass [37, 38].

Latest statistics reveal that approximately 130 million tonnes of glass waste are generated worldwide annually, where a poor recycling rate of only 21% is achieved on average. Furthermore, the USA, Canada, Australia, United Kingdom, Germany and India generate 11.4, 0.75, 1.1, 2.4, 2.5 and 21 million tonnes of glass waste, respectively, each year, with recycling rates of 27%, 40%, 57%, 45%, 80% and 45%, orderly [39]. The Scandinavian countries of Norway and Sweden, as well as Belgium and Germany, can be identified as the leading nations with respect to recycling glass, achieving recycling levels of around 80% [40], with the majority of countries trailing far behind. In addition, China is identified to be the country that generates the largest amount of glass waste, where approximately 46 million tonnes are disposed into landfill sites each year. Furthermore, it is reported that less than 30% of the waste glass generated is recycled [41], thus portraying the need for improvements in schemes for the management of glass waste. The state of Victoria, Australia, where the current testing is undertaken, itself is responsible for producing approximately 250,000 tonnes of waste glass each year [42, 43], whilst about 50% of this glass waste is stockpiled.

The global recycling rates for a majority of waste materials have shown appreciable improvement over the past decades; however, the recycling rates for glass have lagged behind, showing comparatively less progress. A sizeable portion of glass items undergoes breakage during collection and transportation to the recycling facility. Following the breakage, glass containers bearing different colours get mixed with other waste materials, making it impossible to separate them from other waste contaminants. An additional challenge to achieve higher rates of glass recycling has been the availability of a variety of glass types having disparate chemical compositions, with some having hazardous classifications. The aforementioned reasons have been identified as some of the major issues that hinder the progress of glass recycling worldwide, thereby having a negative effect on the recycling rates [44–48]. Further to this, glass waste is acknowledged to be non-biodegradable, leading to increased accumulation, thereby posing a serious threat to ecosystems as well as adding a burden on the physical availability of landfill space [49–52].

Although the non-biodegradable property is undesirable for materials placed in landfill sites, this exact property is very much desirable for materials used in construction endeavours. The non-biodegradable nature of the glass helps to maintain its physical properties as well as remain chemically inert over extended periods [53, 54]. Moreover, glass waste has several other properties that enable its use as a construction aggregate, including satisfactory mechanical strength, low water absorption, insensitivity to moisture, good workability (available in a range of well-graded particle gradations) and durability [55–66]. These attributes of

waste glass make it highly appropriate for its application as a supplementary construction aggregate, bringing about a two-fold benefit in the form of providing a solution to the accumulation of glass waste in landfills and also reducing the use of fast depleting high-quality virgin aggregates [67–74].

Several research projects undertaken in the past decade have utilised waste glass to enhance the mechanical performance as well as physical properties of soils having inferior engineering qualities. The introduction of glass to medium–high plasticity clays showed an increase in the maximum dry density (MDD) and a decrease in optimum moisture content (OMC) up to a maximum inclusion of 12% glass, thereby indicating superior compaction and increased workability of clay–glass mixes [75]. The same reveals that the CBR and shear results in terms of the angle of friction also showed improvement with an addition of crushed glass up to 12% glass. The findings from [21] are in agreement, where the MDD increased, and OMC decreased as up to 80% of crushed glass was incorporated into the clay, further reporting that the changes in both MDD and OMC were more pronounced for inclusions of 20–40% glass. The same study revealed that the hydraulic conductivity of the clay was increased as the crushed glass was incorporated into the clay. The introduction of crushed glass to the lateritic soil resulted in an increase in MDD up to 8% glass, whilst adding further glass led to decreasing MDD. Furthermore, the UCS values increased as higher contents of crushed glass were added up to a maximum inclusion of 16%; however, it was observed that the magnitude of the increase decreased as a glass content of greater than 14% was introduced [76]. CBR, UCS, permeability and MDD values showed increasing trends with the introduction of glass cullet for lateritic soil up to a maximum inclusion of 20% glass, whilst the OMC was noted to show a decrease [77]. Testing conducted on black cotton soil–glass powder blends revealed that the OMC decreased whilst the MDD increased up to 4% glass powder (the optimum addition), beyond which a decrease was observed. Additionally, the UCS values increased up to an optimum addition of 4% of glass powder, where the optimum specimen recorded a UCS increment of approximately 350% in comparison to the control black cotton soil specimen. The CBR results, on the other hand, initially showed a decrease with the inclusion of glass powder, where the values decreased up to 4% glass, followed by a significant improvement upon the inclusion of 6% glass powder [78]. The inclusion of glass powder to clay soil had a similar effect on the UCS up to an optimum addition of 6% glass powder, beyond which further increasing the glass powder content up to a maximum addition of 12% led to a decrease in the UCS [79]. Furthermore, the MDD was observed to increase with the inclusion of 12% glass powder, whilst the OMC, on the other hand, decreased with increasing glass content. Although the current study focusses on improving low plasticity clay with the addition of crushed waste glass, existing literature on improving soils using glass fibres indicates the versatility and the potential of using aggregates derived from waste glass in soils [80–82].

Previous studies evaluating the efficacy of glass in clay improvement have primarily focussed on powdered or fine soda-lime glass. Although some existing studies have evaluated the improvement in strength characteristics of clay with granular CG, a majority of the studies have focussed on the improvement in compressive strength characteristics or the reduction in swell–shrink properties. Little emphasis has been made on how the addition of granular glass affects the resilient properties. Furthermore, there is an even greater lack of research that undertake microstructural and physicochemical studies such as microCT, scanning electron microscope (SEM), X-ray fluorescence (XRF), X-ray diffraction (XRD) and soil–water characteristic curve (SWCC) tests which enable a better understanding of the mechanisms by which the addition of CG affects the strength and resilience properties. Further to this, it can be seen that there is a lack of literature that studies the suitability of improving low plasticity clay using recycled crushed glass for application in the subgrade layer of roads. Thus, the current study entails a comprehensive evaluation of the effect of introducing granular CG to a low plasticity clay, covering aspects of mechanical strength, resilient characteristics, microstructural properties, physicochemical properties and the behaviour pertaining to interaction with moisture, with the main focus set on evaluating the potential for a low plastic clay improved with crushed glass to be utilised as road subgrade.

2 Materials

2.1 Clay Soil and Recycled Crushed Glass

The low plasticity clay used in this research was acquired from a road development project site located in the suburb of Werribee, the state of Victoria, Australia. The exact location for the pick-up and location with reference to Melbourne CBD is presented in Fig. 1. According to the Geological Survey of Victoria's 1:63 360 Scale Melbourne geological map, the site's surface geology consists of Quaternary-age flood sediments "Deutgam silt" overlying Quaternary-age "Newer Volcanics" Basalt. The clay soil was collected at a depth of approximately 1.5–2.5 m, where the method of collection could be classified as the disturbed state. The pick-up location was determined following careful scrutiny of the area along with the proposed plan by the City of Wyndham as presented through the council plan for the years 2021–2025 [83]. The area governed by Wyndham Council was identified to be a fast-growing suburb with a local population growth rate of 4.7% recorded for the year
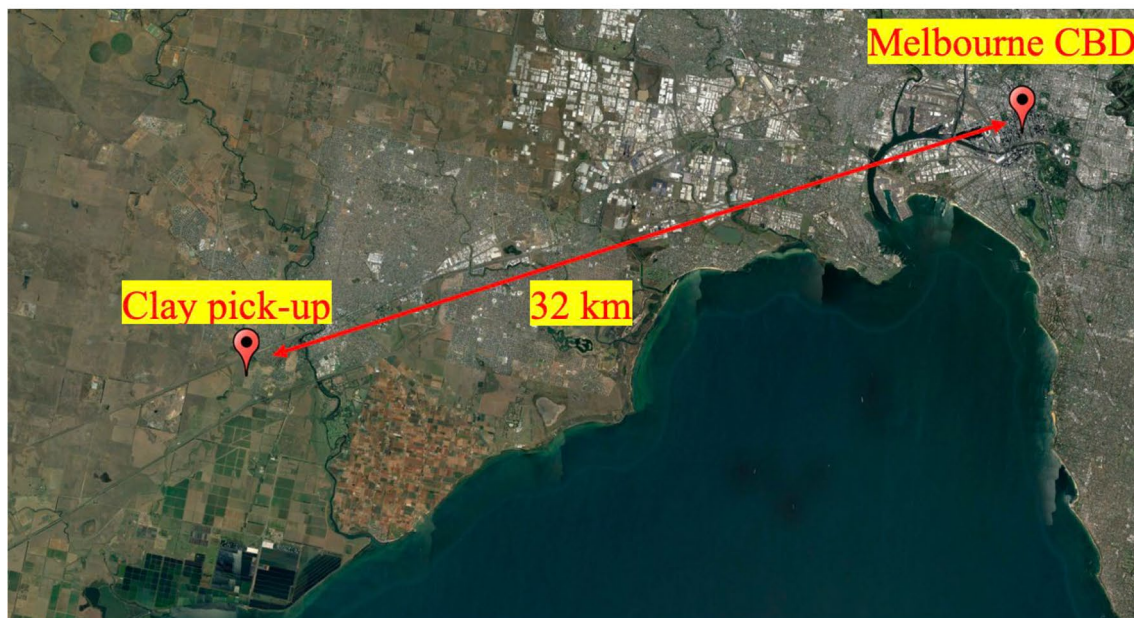
**Fig. 1** **a** Location of soil pick-up and **b** clay pick-up location with reference to Melbourne CBD

2020 according to the council plan. Furthermore, as per the council plan, the local population is expected to increase from the estimated value of 283,000 recorded in the year 2020 to a staggering 500,000 by the year 2040. Such a drastic increase in population, without doubt, requires significant developments in terms of roads and various other essential infrastructures within the locality. Focussing on road infrastructure, in particular, it could be deemed that an increase in the local population of this extent would require the development of many local streets, arterial roads and the expansion of existing road infrastructure in order to sustain the level of growth. In addition to this, the increased usage of the road networks by the local residents would hasten the deterioration of the current road network, resulting in the

Table 1 Physical characteristics for the low plasticity clay and CG

Properties	Low reactive clay	Crushed glass	Standard
Passing no. 200 sieve (%)	85.8	4	[91]
Sand content (%)	14.2	96	[91]
Silt content (%)	15.5	4	[91]
Clay content (%)	70.3	0	[91]
Liquid limit (%)	29.3	–	[92]
Plastic limit (%)	20.5	–	[92]
Plasticity index (%)	8.8	Non-plastic	[92]
Swell–shrink index, I_{S-S} (%/pF)	1.67	–	[93]
Soil classification	CL	SP	[94]
Specific gravity (G_s)	2.62	2.64	[95]
Linear shrinkage (%)	3	–	[96]
Maximum dry density (MDD) (t/m^3)	1.77	1.73	[97]
Optimum dry density (OMC) (%)	15.94	10	[97]
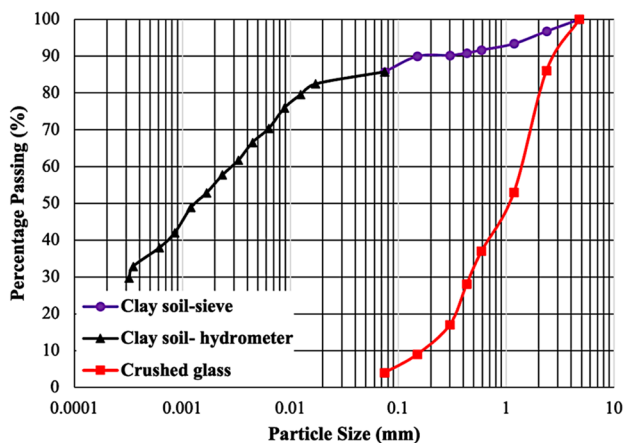
Fig. 2 Particle size gradation for low plasticity clay and crushed glass

Table 2 XRF data for the low plasticity clay and crushed glass

Oxides	Low plasticity clay (%)	CG (%)
SiO$_2$	61.26	68.14
CaO	0.68	14.15
Na$_2$O	–	12.51
Al$_2$O$_3$	21.55	2.18
MgO	1.06	0.74
Fe$_2$O$_3$	11.55	0.92
SO$_3$	0.05	0.09
TiO$_2$	0.68	0.12
P$_2$O$_5$	0.36	0.24
K$_2$O	1.29	0.54
Cr$_2$O$_3$	0.03	0.11
MnO	0.04	0.03
ZnO	0.1	0.03
V$_2$O$_5$	0.04	–
NiO	0.02	0.01
CuO	0.01	0.01
Rb$_2$O	0.01	–
SrO	0.01	0.03
ZrO$_2$	0.07	0.03
Nb$_2$O$_5$	0.01	–
BaO	0.05	–
PbO	–	0.03

roads reaching their end of service life in a shorter span of time. Thus, it was deemed that the soils within the locality are ideal to be utilised in this study, thereby increasing the relevance of the research as well as its possible in-field implementation within the locality and beyond. The soil can be classified as a low plasticity clay, with a plasticity index of 8.8% and a swell–shrink index value (I_{S-S}) of 1.67%/pF.

The supplementary additive considered in the study was crushed glass (CG) with a maximum size of 5 mm. The crushed glass is processed at a local recycling facility where glass bottles and other recyclable glass items are ground down to achieve a particle distribution of ~ 5 mm. The CG consists mainly of sand-sized particles, although a limited fraction of silt-sized particles is present [84].

Table 1 introduces the physical characteristics pertaining to the clay as well as the crushed glass utilised as the supplementary additive. Figure 2 presents the particle size gradations for clay as well as CG. It is noteworthy that results relating to the particle size distribution have been obtained through two separate tests, namely mechanical sieving [85] and hydrometer analysis [86]. Table 2, on the other hand, provides information on the elemental make-up of both the low plasticity clay as well as the CG as determined by the X-ray fluorescence (XRF) test carried out using the Bruker Axs S4 Pioneer. Furthermore, the X-ray powder diffraction (XRD) testing was carried out on oven-dried clay and CG
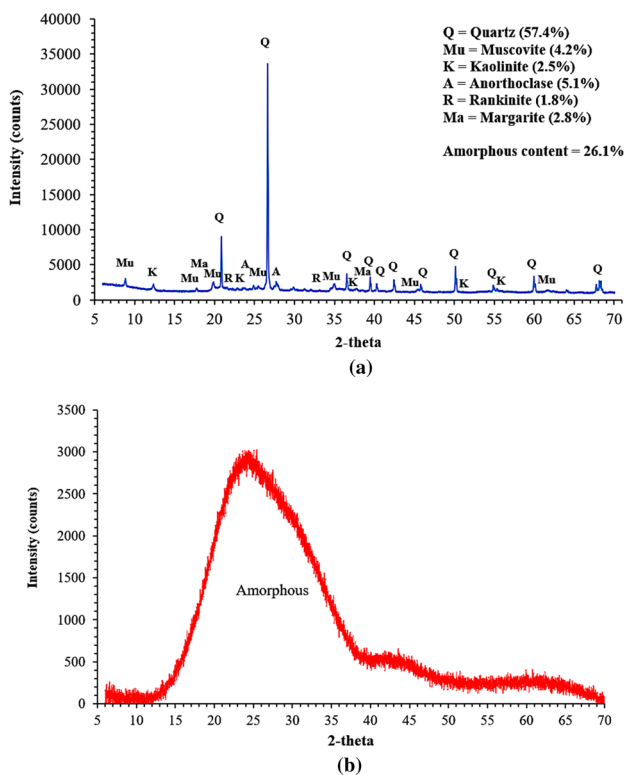
Fig. 3 XRD results for **a** low plasticity clay and **b** crushed glass

powder specimens using AXS D4 Endeavour fitted with the lynxeye linear strip detector and Cu-Kα radiation source. The voltage and current settings were 40-kV and 40 mA, respectively. X-ray diffractograms were collected between 5° and 70° 2-theta with a step size of 0.01° and a counting time of 0.5 s per step. Figure 3 provides the various phases pertaining to the respective mineralogy of each specimen as identified by the XRD analysis. The clay utilised in the research is observed to contain high amounts of quartz, muscovite, kaolinite, anorthoclase, rankinite and margarite, as shown in Fig. 3a. The soil used in the experiment was naturally composed of sand and the clay minerals mentioned afore. Semi-quantitative phase analysis (Fig. 3a) was carried out using Bruker TOPAS software and COD crystal structure database [87]. The crushed glass is found to consist of amorphous material overall, as reflected in Fig. 3b. The glass is typically amorphous in nature [88–90] which is evident from the broad, amorphous hump in the XRD diffractogram [91–97] (Fig. 3b).

3 Specimen Preparation and Procedure for Testing

In the current study, both the low plasticity clay and CG were initially oven-dried at a temperature of 105 °C for a minimum period of 48 h to remove all existing moisture and achieve a fully dry state. The crushed glass was then introduced and mixed into the clay in five distinct percentages of 0, 5, 10, 15 and 20% with respect to the dry weight of clay. It is worthy of note that the oven-dried soil was crushed utilising a mechanised soil crusher to disintegrate the lumps of clay, allowing for the glass to be uniformly distributed in the clay. The addition of CG to the clay leads to a change in the clay matrix, thereby arising the need for compaction testing to establish the optimum moisture content (OMC) at which the maximum dry density (MDD) could be achieved. Standard compaction testing was implemented in this research which is in line with the requirement for subgrade clay. The standard compaction testing was performed as per the guidelines of the Australian standards [97] for each different clay-crushed glass mix. All mechanical strength and resilience test samples were prepared at their respective OMCs. It is also noteworthy that pre-curing of specimens was required in accordance with [98] for the said mechanical strength and resilience tests, including standard compaction, UCS, CBR, resilient modulus, shrinkage and swelling, etc. According to the standard, the soil specimens have to be allowed to pre-cure in sealed containers for a set period of time following the mixing at OMC. The period of time for which the specimens should be kept aside for pre-curing is dependent on the liquid limit of the clay. The curing period allows the clay particles to effectively absorb the free water available. The standard [98] articulates that a 24-h minimum pre-curing period is required for clays with a liquid limit (LL) of less than 30%. Since the LL of the clay is 29.3%, a minimum pre-curing period of 48 h in sealed plastic bags was adopted in this study to ensure adequate time for absorption of free water. The compaction test was initially conducted on each distinct specimen for a range of moisture contents following the 48-h pre-curing period, where each specimen was compacted into 3 separate layers within a cylindrical steel mould of 115.5 mm in height and 105 mm in diameter, with each layer receiving 25 blows from a standard compaction hammer of 2.7 kg dropping from a height of 300 mm [97].

All mechanical and resilience test specimens (as mentioned above) were prepared by adding in the relevant glass contents and mixing thoroughly at OMC using a

mechanical mixer for 5 min until a homogeneous mixture was achieved. These specimens were then sealed off in plastic bags and left to cure for a minimum of 48 h. Following the curing period, the mixtures were subjected to standard compaction effort and tested immediately. It is worthy of mention that three replicate samples were prepared for all mechanical tests with respect to each mixture composition, and the average results of the tests were reported.

UCS specimen preparation was undertaken in accordance with the Australian standard [99], where the specimens were compacted in three layers, with each layer receiving 25 blows from the 2.57 kg standard compaction hammer. The mixtures were compacted in a steel UCS mould of 115.5 mm height and 105 mm diameter, with an extension collar of 50 mm height attached. Excess soil was then trimmed, and the specimens were then extruded from the mould immediately using a mechanical extruder. The extruded specimens were then tested using the Shimadzu 50 kN universal testing machine at a loading rate of 1 mm/min.

CBR test is a widely acknowledged penetration test that assesses the stiffness and rigid nature of a pavement layer [100]. Unsoaked CBR testing was conducted as per the guidelines in the Australian standard [98]. The CBR specimen was compacted in a steel mould with an internal diameter of 150 mm and a height of 180 mm. A steel spacer of a height of 60 mm was placed at the bottom of the base plate, and the mould was then fitted onto a flat base plate. The mould also comprised an extension collar of height 60 mm, which was fitted in place on top of the mould. Every specimen was compacted into 3 separate layers, each layer getting 53 blows from the 2.57 kg standard compaction hammer. The extension collar was then removed, and excess soil beyond the mould was trimmed off. The mould containing the compacted specimen was then lifted off carefully and flipped over, at which point the surcharge weights were placed on top of the CBR specimen, and the CBR testing was conducted right away at a fixed rate of penetration of 1 mm/min.

The repeated load triaxial (RLT) test provides a vital evaluation of the performance of a road layer. The RLT test involves the application of a series of sequences with repetitive impulse load cycles on the specimens. These impulse loads closely mimic on-going wheel loadings of vehicular traffic as experienced by road aggregate, thus, allowing to achieve a better understanding of the performance of a soil concerning its stiffness [101]. The RLT testing in this study was carried out in accordance with the standard [102]. The specimen compaction was performed in a steel cylindrical split mould of 200 mm in height and 100 mm in diameter.

The compaction took place in 3 separate layers; each layer received 40 blows from the standard compaction hammer, then excess soil was trimmed, following which the split mould was loosened to free the specimen. This specimen was then inserted into a rubber triaxial testing membrane with the aid of a low-suction air pump and membrane stretching funnel. The specimens were then placed in the DTS-16 repeated load triaxial cell setup, which was utilised to carry out the RLT testing. The test was performed under a sequence of loads with several cycles of varied magnitude impulse loading. The loading pulse form implemented in the test was of haversine shape with a loading–unloading sequence interval of 0.1 s loading followed by 0.9 s unloading.

The swelling–shrinkage specimen preparation was carried out by first dry mixing the soil and crushed glass (CG) until the CG was thoroughly mixed in with the soil. Then a water content of 16% was introduced to all mixtures, followed by a thorough mix. The homogenous mix was then promptly transferred into plastic bags, sealed off and set aside for a curing period of 48 h.

The swelling–shrinkage procedure is a combination of two separate tests, one in the form of swelling and the other in the form of shrinkage. Concerning the preparation of the specimens for the swell test, each specimen was compacted in a UCS mould in a single layer, consistent with the requirements to achieve standard compaction. A thin film of Vaseline was applied on the inner surface of the consolidation cells cutting ring, following which the cutting ring was driven into the specimen, at which point any excess material was trimmed from the top and bottom sides of the cutting ring using a spatula to obtain a smooth and flat specimen. The swell test was conducted, satisfying the requirements of the Australian standard [93], utilising a consolidation cell set-up.

The shrinkage specimens were prepared in accordance with the Australian standard [93], by first compacting the specimen in the UCS mould and driving a core tube with an internal diameter of 38 mm into the specimen by gently tapping the tube using a rubber mallet. The specimen deposited in the core tube was then extruded with the aid of a plastic plunger and trimmed to a length that is 1.5–2 times the diameter. A detailed evaluation of the development of the Australian standards pertaining to the swelling–shrinkage test can be found in [103], whilst further details on the testing procedure can be obtained through [104].

Given the significance of understanding the interaction between the low plasticity clay and moisture, the soil–water characteristic curve (SWCC) test was conducted on the control clay specimen as well as the specimen mixed with the

optimum glass content. It is noteworthy that both the clay and the CG were first sieved with a 1 mm sieve when preparing the SWCC samples, as the samples were required to have a height of 5 mm to be placed within the WP4 machine steel cups. Specimen preparation was carried out for a range of moisture contents, and all specimens were placed in sealed plastic bags for a curing period of 2 days. The compaction of the specimens was performed within the confinement of a UCS mould, where a single layer was compacted using 25 blows from the standard compaction hammer. It is noteworthy that care was practised to achieve a uniform density across all specimens. Following the compaction, the extruding of a manageable sample size was achieved by driving a cutting ring bearing a diameter of 50 mm and a height of 25 mm into the specimen using a rubber mallet. Studies that are currently available on SWCC have used a similar technique for specimen extrusion [105]. The specimens were then trimmed using a spatula, where care was exercised to achieve a constant height of 5 mm to allow its fitting within the steel WP4 machine cups having a diameter and height of 27.5 mm and 8 mm, orderly. A constant height of 5 mm was achieved to minimise the influence of the specimen thickness on the SWCC values [106]. It is worthy of mention that the results used in the study were obtained by averaging that of three specimens at each moisture content, thereby improving the reliability of the results. The testing was carried out with the use of the WP4C Dewpoint Potentiometer employing the "precise mode", thus allowing for results with a higher degree of accuracy to be obtained. The specimens were weighed immediately post-testing and oven-dried for the purpose of determining the moisture content. It is noteworthy that a potassium chloride (KCl) solution of concentration 0.5 Molal/kg was used to calibrate the WP4 as per the guidelines in the manual provided by the manufacturer. Additional information pertaining to the dewpoint potentiometer can be found in [107].

The scanning electron microscope (SEM) and X-ray microcomputed tomography (microCT) analyses were employed to assess how the addition of CG influences the microstructure of the soil blends. The specimens required iridium coating prior to being subjected to imaging via the use of SEM equipment to increase surface conductivity, reducing the build-up of charge on the specimen surface, thereby enabling the capturing of higher quality images that depict a greater depth of visual and surficial features. The iridium coating was performed with the use of the Leica EM ACE600 Sputter Coater equipment, whilst the SEM imaging was obtained using the FEI Quanta 200 device operated at a voltage of 20 kV. The X-ray microCT imaging was carried out utilising the Bruker Skyscan 1275 X-ray microcomputed tomography equipment. The microCT analysis is useful in evaluating how the addition of glass affects the internal porosity and the microstructural alignment of the
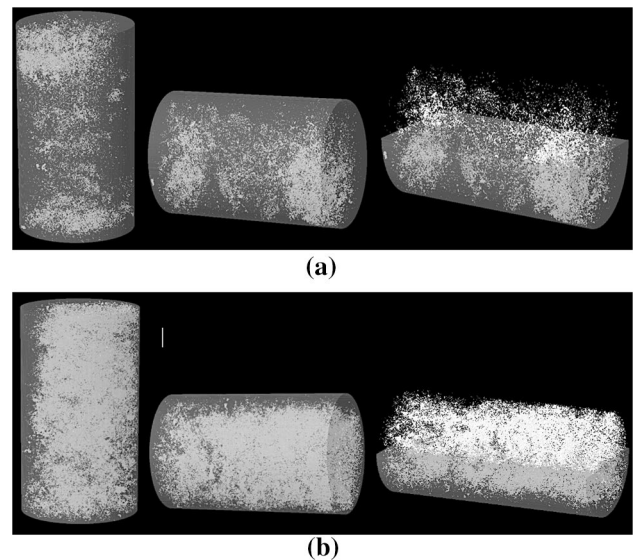

Fig. 4 MicroCT 3D images for **a** control specimen and **b** clay with 15% CG

Table 3 Porosity results from X-ray microCT analysis

Specimen ID	Closed porosity (%)
Low plasticity clay control	2.25
Low plasticity clay with 15% CG	5.30

low plasticity clay. The X-ray microCT specimens were prepared by first compacting them in a UCS mould followed by extrusion using a core tube with a diameter of 25 mm to form cylindrical specimens with a diameter of 25 mm and a height of approximately 30 mm. The microCT scans were performed with the copper filter attachment and the X-ray source operating at its maximum output, which is a tube voltage value of 100 kV and a current of 100 μA. The internal structure, as well as the surficial features of the specimen, are presented through an image that is formed based on the intensity of the X-rays that are reflected and deflected from the specimen and distinguished by the detector. This image is the combination of several hundred slices of image, where every slice has a thickness of 25 μm. For instance, the scan of a specimen of height 30 mm with the step rotation set at 0.2° will contain 1200 individual slices of image.

4 Results and Discussion

4.1 X-Ray Microcomputed Tomography (MicroCT) and Scanning Electron Microscope (SEM)

3D images for the low plasticity control clay and low plasticity clay containing 15% CG obtained through the X-ray microCT analysis are provided in Fig. 4a, b, orderly. The images depict closed pores located within the specimens in white colour whilst the solid volume of the specimens is shown in grey colour. The specimen including 15% CG was chosen for conducting both SEM and microCT as it was decided as the glass content that best enhanced the overall mechanical properties of the clay. Upon a quick glance at the images, it is clearly evident that the introduction of glass into the clay resulted in an increase in porosity as manifested by the more pronounced white colour (closed pores). A statistical comparison of the increase in porosity induced by the addition of 15% CG is presented in Table 3, revealing that the closed porosity increased by approximately 3% with the introduction of CG, with the value increasing from 2.25% for the control clay to 5.30% for the specimen with 15% CG. The heightening of the porosity upon adding CG could be elucidated through the larger particle size of CG, which reduced the efficiency of compaction. The permeability is a vital parameter when considering pavements [108, 109], where the drainage function of the subgrade layer is dependent on its degree of permeability. A subgrade with very low permeability (poor drainage function) can impede the draining of water out of the pavement, leading to stagnation of water within the pavement system. Hence, it is important for the subgrade layer to have adequate drainage. Such accumulation of water within the pavement can have a detrimental effect on the longevity and performance of the road [110–112]. This drainage function (hydraulic conductivity) is associated with the degree of porosity [113, 114]. Materials with higher porosity lead to better drainage [115]. Thus, it can be deemed that the introduction of CG into the clay aids the subgrade layer in achieving a higher level of hydraulic conductivity, preventing the inundation of the pavement during heavy rainfall. The SEM analysis results provided in Fig. 5 attest to these findings. Upon drawing a comparison concerning Fig. 5a, b, which shows SEM results for the control clay and specimen with 15% CG, orderly, it is evident that the larger particle size of glass led to increased porosity. Furthermore, SEM imaging reveals rough, jagged/irregular features for the CG. This is a result of the mechanical pulverisation of the glass in the recycling facility. Such features allow for increased contact points for particle attachment through mechanical interlocking leading to enhanced resistance to sliding of particles, hence improved interlocking of the soil matrix.

4.2 Standard Compaction Results

The two critical findings from the compaction test, i.e. the optimum moisture content (OMC) and maximum dry density (MDD) of the control low plasticity clay specimen as well as the clay–glass blends, are presented in Fig. 6. As depicted in the figure, the control specimen for the clay recorded an OMC of 15.94%, which is observed to decrease slightly upon the introduction of CG, where the addition of 20% CG was noted to decrease the OMC to a value of 15.41%. This minute decrease in the OMC of the clay as a result of the incorporation of CG could be interpreted by the relative insensitivity to the moisture of the glass aggregate, thereby reducing the water absorption potential of the clay blends. The OMC results are in line with the findings from previous studies where glass was used to stabilise clay [79, 116].

The MDD, on the other hand, showed an opposing trend to OMC with the introduction of glass as expected, where the MDD was observed to increase slightly from 1.77 to 1.82 t/m^3 with the addition of 20% CG. This could be explained by the increased workability brought to the blends by introducing glass, which is evident through the slight reduction in OMC with the addition of glass [117, 118]. Interestingly, although there is an overall increase in MDD, there is no change in MDD with the addition of 5% CG, whilst the increase in MDD initiates with a CG content of 10% and greater. A probable explanation for the unchanged MDD at the start could be because CG and the low plasticity clay have close density, and the soil–glass interaction almost completely dominates, leading to high frictional resistance and, thus, poorer settlement. The reduced settlement may lead to unaffected MDD. However, the increase in glass content could cause a shift in the interaction in favour of glass–glass interaction, at which point glass particles gain more freedom of movement within the specimen as the compaction occurs, thereby aiding in increasing the MDD value of the clay–glass blends.

4.3 Unconfined Compressive Strength Results

The unconfined compressive strength data for low plasticity clay–glass blends are shown in Fig. 7. Upon viewing the data, it is evident that the UCS values increased with the introduction of CG up to an optimum inclusion of 10% CG, where the UCS is noted to increase to a value from 258.39 kPa for the control clay to 287.83 kPa for the specimen with 10% glass. This increase in the UCS with the introduction of up to 10% glass could be attributed to the high angularity of the glass aggregate as well as the granular size of the glass, as observed in the SEM analysis results. High angularity is associated with greater contact surfaces for efficient frictional interaction of soil–glass particles as

Fig. 5 SEM images of **a** control clay specimen and **b** clay with CG
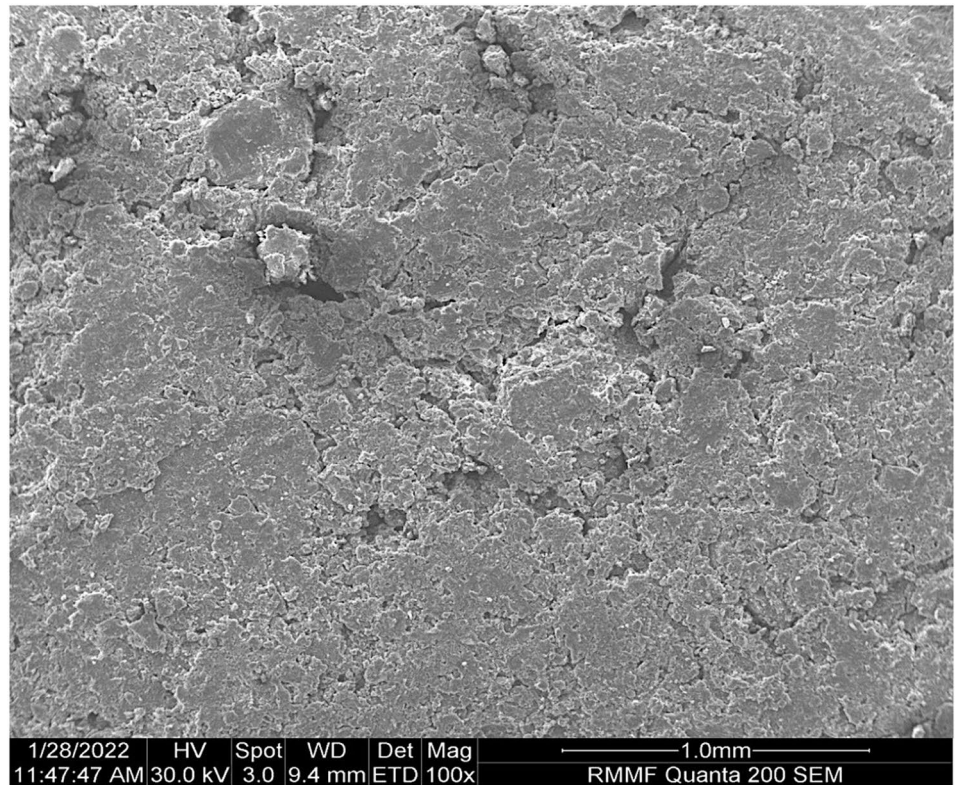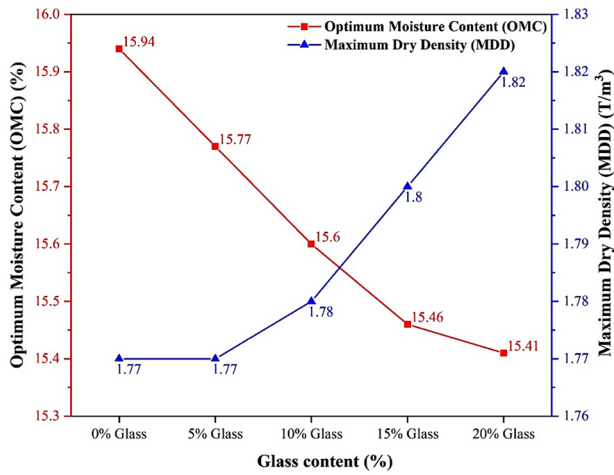

(a)
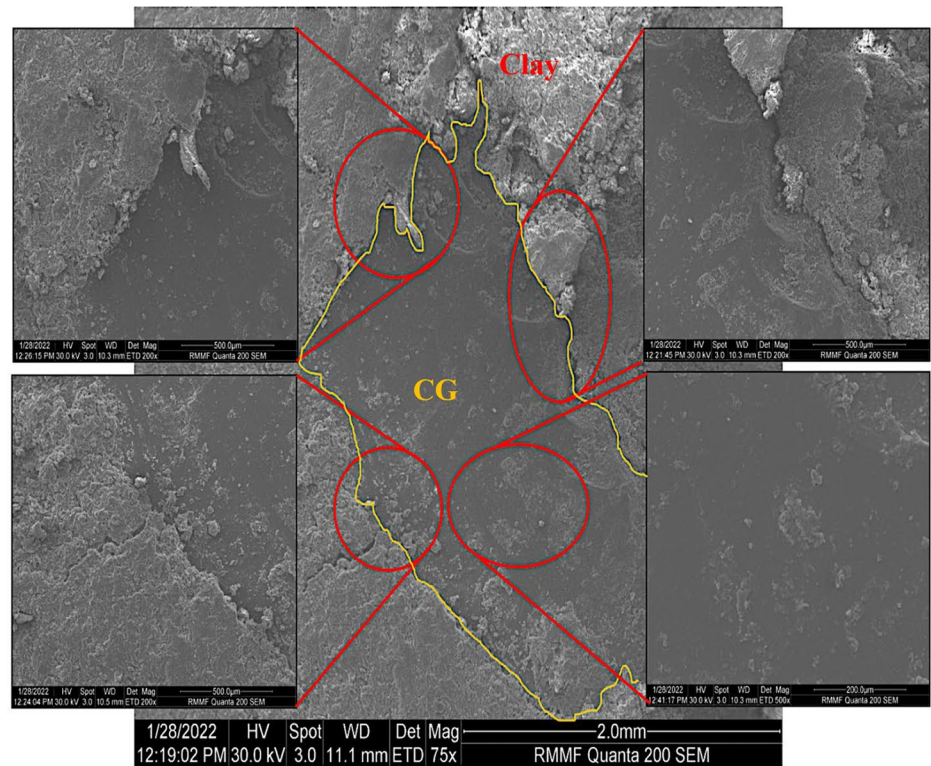
(b)

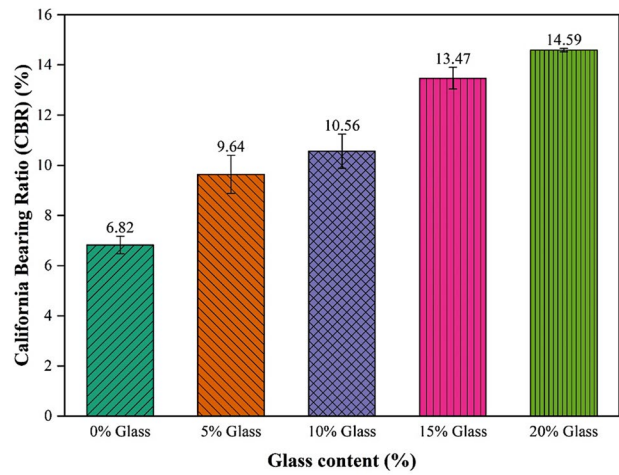**Fig. 6** Influence of CG on MDD and OMC of the low plasticity clay blends

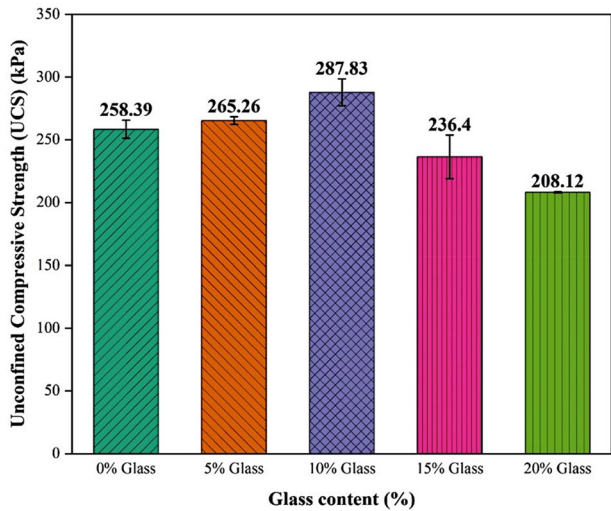**Fig. 8** Influence of CG on CBR values

Fig. 7 Influence of glass on UCS of low reactive clay blends

well as improving the mechanical interlocking of aggregates, thereby enabling better resistance to particle sliding. It is also important to note that the UCS values increased when the CG content was increased from 5 to 10%; this could be explained by the more effective soil–CG interaction due to the higher addition of glass, leading to an increase in the surface area of glass available for interaction with the soil. However, further increasing the CG content to 15 and 20% led to reduced UCS values of 236.39 and 208.12 kPa. As more glass is introduced, the increased presence of glass promotes a higher degree of CG–CG interaction. CG is known to be a material with low cohesion, whilst clay, on the other hand, is a highly cohesive material. Thus, an increased CG–CG interaction instead of the desired CG–clay interaction would, in turn, lead to reduced frictional forces. A

reduction in the frictional forces leads to a material that is more compressible; thus, a reduction in the UCS values can be observed as a CG content greater than 10% is introduced to the clay. In addition, greater introductions of glass led to an increase in the voids, as observed through the porosity results from the microCT test; this is due to the larger particle size of the glass. This is especially the case with higher glass contents due to the increased glass–glass interaction. Similar findings were reported in studies conducted on soil–glass blends in the past [119, 120].

4.4 California Bearing Ratio (CBR) Results

The change in CBR values caused by the introduction of CG to the clay is graphically represented along with standard deviation error bars in Fig. 8. As observed from the figure, the control clay specimen recorded a modest CBR value of 6.8%, whilst this value increased to 9.6, 10.6, 13.5 and 14.6% with the addition of 5, 10, 15 and 20% CG, respectively. Furthermore, it is worthy of mentioning that the most significant improvement in CBR is observed as the CG content is increased from 10 to 15%, whilst a further increase in CG to 20% led to a far less improvement. The CBR is a penetrative-compaction test that provides an indication of a specimen's ability to resist sliding forces (shear resistance); therefore, the enhancement of CBR values due to the addition of CG could be explained through the granular size and angularity and irregular shape of the glass particles, which provides improved mechanical interlocking between clay and glass particles, leading to greater frictional forces between the clay and glass, thereby improving the effectiveness of specimen in resisting sliding/compressive forces [121, 122]. This being said, the reduction in the magnitude of improvement as CG is increased from 15 to 20% is due to the increased presence of glass, where CG–CG interaction starts to take a

greater effect over the more desirable CG–clay interaction. This results in increased sliding of glass particles past one another as glass has low cohesion, thus has a lower ability to frictional resistance against sliding forces, which is consistent with the observations concerning UCS values from the previous section. Studies conducted in the past on lateritic soil improved with glass in [76, 123] also reported improvements in CBR up to optimum inclusions of glass.

The maximum UCS being achieved at 10% whilst the CBR continued to increase although at a diminishing rate. This can be explained through the nature of the two tests. The UCS is a pure compression test performed on an unconfined specimen where the loading is applied on the entire specimen, whilst the CBR test is a penetration test involving a plunger being driven into a test specimen that is confined within the CBR mould. Given the nature of the CBR test, it gives a reflection that is based more on the internal shear performance and frictional resistance of the specimen; the plunger pushes a portion of the sample down, where this portion has to overcome internal friction, as opposed to the UCS test which gives a reflection of the ability of the entire specimen to resist compression. With the addition of CG, the mechanical interlocking increases because of the CG–clay interaction as the CG is jagged in nature, whilst at higher inclusions of CG, the less desirable CG–CG interaction becomes more prominent, which causes a reduction in the ability to resist compressive forces due to CG having low cohesion. However, given that the CBR testing is performed within the confinement of the mould (preventing lateral movement), the improved mechanical interlocking brought about by the jagged CG could play a more vital role than it does in the case of UCS. Thus, the CBR continues to increase with the increasing CG content, although the magnitude of the increase can be observed to diminish as greater than 15% CG is introduced. This decrease in the magnitude can be explained through the increased CG–CG interaction.

4.5 Swelling–Shrinkage Results

Swelling–shrinkage test results are provided in Fig. 9, showing the variation in swelling strain, shrinkage strain and swell–shrink index with the introduction of distinct percentages of CG. It can be observed that the inclusion of CG resulted in the decrease of swelling strain, shrinkage strain as the well as swell–shrink index. The control clay specimen recorded swelling strain, shrinkage strain and swell–shrink index values of 1.74, 2.14 and 1.67%/pF, respectively, whilst the specimen containing 20% CG recorded respective values of 1.06, 1.46 and 1.10%/pF. Decreasing swell–shrink values could be elucidated by replacing clay that has a relatively high affinity to water with CG that is mostly non-expansive silica and, thus, insensitive to water [124]. Another factor that could contribute to a lesser degree to the decrease in the swell–shrink parameter is the angular nature of the glass that prevents the swelling of the soil by forming an effective interlocking mechanism in the soil. This resulted in providing resistance to heaving and shrinkage of low plasticity clay due to the inclusion of CG. The findings from the testing are consistent with results from [76, 119, 125].

4.6 Soil–Water Characteristic Curve (SWCC)

Several studies conducted in the past have highlighted the efficacy of using Decagon's WP4 Dewpoint PotentiaMete to swiftly acquire reliable soil suction data and the soil–water retention behaviour [104, 126, 127]. The soil–water characteristic curve (SWCC) derived using the
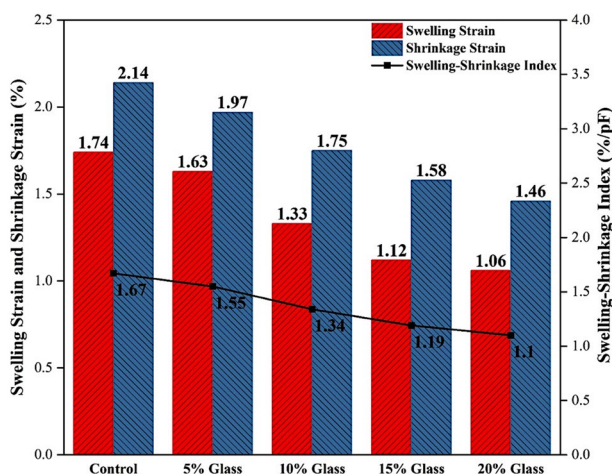
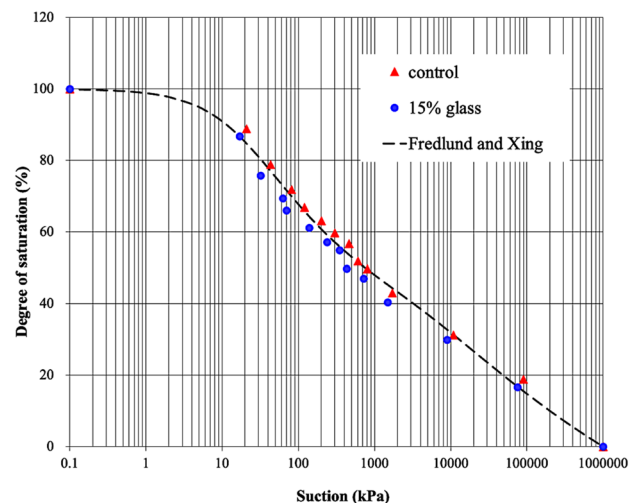**Fig. 9** Swelling strain, shrinkage strain and swell–shrink

Fig. 10 Degree of saturation versus soil suction for control clay and the specimen containing 15% glass

WP4 machine can be observed through Fig. 10, where the results have been fitted into the equation developed by Fredlund and Xing [128]. The start and end points of the curve were adopted as the limits. It can be discerned through Fig. 10 that the control clay specimen was predominantly found to be above that of the specimen containing 15% glass. Thus, presenting that the inclusion of recycled glass to the low plasticity clay leads to an overall decrease in the soil's capacity to retain water. Findings that are consistent with those of the current study are reported by [129]. In addition, the SWCCs of both specimens can be seen to be of the unimodal form, thereby suggesting the presence of only one level of pore size, as the presence of multiple pore sizes would result in the SWCCs exhibiting bimodal features [130]. These unimodal-formed SWCCs imply that the addition of up to 15% glass does not have a significant influence on the distribution of void sizes within the specimen. Given its low capacity for water

absorption, introducing glass to the clay that has a considerably higher capacity of water absorption undoubtedly leads to a change in the clay–glass mixture's water absorption capacity. The soil suction decrease due to adding 15% glass can be elucidated through a low ability of water absorption of the clay–glass mix in comparison to the control clay, allowing the clay–glass mix to expel water with relative ease. In addition to this, the degree of porosity has an impact on the SWCC [131], where its effect is heightened at lower values of suction. As observed in Table 3, the increase in the porosity with the addition of 15% glass could also contribute to the decrease in the soil suction.

4.7 Resilient Modulus (M_r) Results

The fluctuations in the resilient modulus (M_r) under the different stress stages for the specimens are graphically represented in Fig. 11a. Figure 11b is a bar chart depicting the average M_r for 15 stages of stress, including the standard deviation in the form of error bars for the specimens of the control clay as well as mixtures containing CG. The overall resilient modulus is noted to increase with the inclusion, up to an optimum inclusion of 15% CG, where the highest M_r of 81.13 MPa was recorded. The improvement in the M_r with the introduction of granular CG could be elucidated in a manner similar to the CBR findings from the previous section. Crushed glass is highly angular (jagged) in nature, which enables efficient interlocking, thereby allowing the soil–glass matrix to resist larger forces with reduced deformation. Another factor could be the irregular surficial features of CG, as observed in the SEM results; such features help to improve frictional resistance against settlement. However, the further increase of CG to 20% led to a decrease in M_r to 74.92 MPa, although the specimen still records a higher M_r than the control clay. The decrease in M_r as the CG content increased beyond 15% could be due to the gathering of glass due to increased CG inclusion, which increased the possibility of glass–glass interaction, thereby leading to a decrease in specimen's ability to resist settlement. The decrease in the specimen's ability to resist settlement is due to CG particles having very low cohesion and thus can slide past one another with relative ease. In fact, a higher proportion of crushed glass can alter the interparticle force chain of the low plasticity clay and reduce the adhesion of the clay soil. The trends reported for the resilient modulus values of clay supplemented with glass in [121, 132] are comparable to that of the current study.

According to the stress levels of the RLT test for obtaining the resilient modulus of clay subgrades, the initial five stages were conducted at a confining stress of 41.4 kPa, whilst this value was decreased once upon the completion of five stages, with the final five stress stages conducted at a confining stress of 13.8 kPa. Keeping the aforementioned in mind and analysing the trends from Fig. 11a, it is possible to articulate that
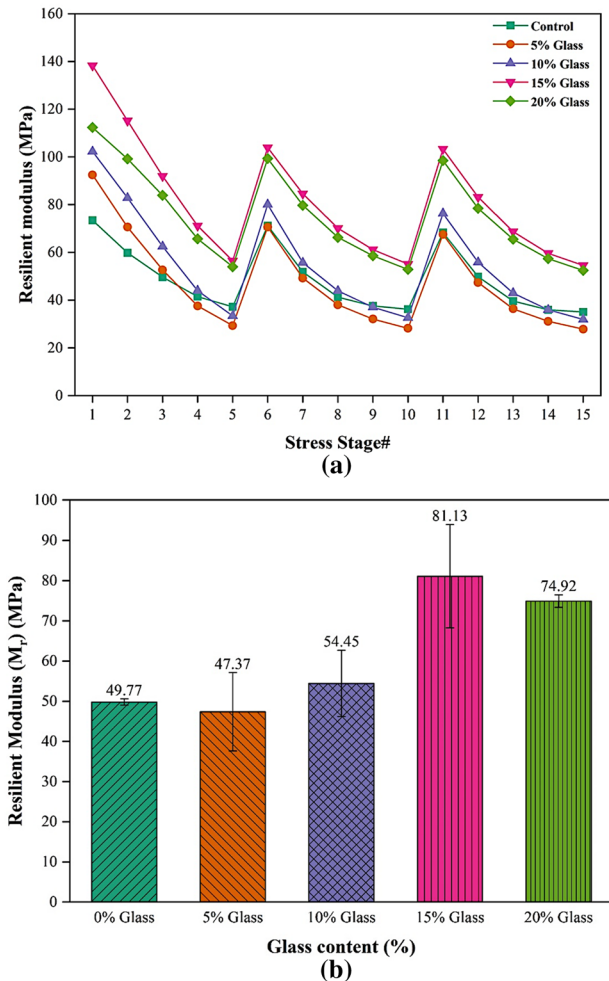

Fig. 11 a Fluctuation of M_r at different stress stages for CG–low plasticity clay blends and b average M_r values for different percentages of crushed glass

increasing the confining stress led to a higher M_r. This is predominantly because of the densification of the clay specimen during the testing procedure as settlement occurs. This reduces the presence of voids within the specimen and improves stiffness properties, consequently increasing the M_r. Conversely, the increase in deviator stress whilst keeping the confining stress fixed led to a reduction in the M_r. This is a stress-softening behaviour which is shown by fine-grained soils of the subgrade [133]. As a result, it is fair to deduce that the deviator stress has a more profound impact on the M_r than the confining stress on the clay subgrade blends. Similar findings concerning subgrade soil were reported by [134].

Several models have been proposed to predict/model the M_r of clay subgrades through the RLT test results. In this study, two models of (a) the generalised model recommended by the Mechanistic-Empirical Pavement Design Guide (MEPDG) (AASHTO 2008) [135] (Eq. 1), and (b) Witczak and Uzan model [136] (Eq. 2) were used for modelling the M_r of the specimens. As can be seen from both models, the M_r relates to the deviatoric stress (σ_d) and confining stress ($\sigma_3 = \sigma_c$).

$$M_R = k_1 P_a \left(\frac{\theta}{P_a} \right)^{k_2} \left(\frac{\tau_{oct}}{P_a} + 1 \right)^{k_3}, \tag{1}$$

$$M_R = k_1 P_a \left(\frac{\sigma_{sum}}{P_a} \right)^{k_2} \left(\frac{\tau_{oct}}{P_a} \right)^{k_3}, \tag{2}$$

where k_1–k_3 are the regression parameters, and P_a is the atmospheric pressure; $\sigma_{sum} = \theta = \sigma_1 + \sigma_2 + \sigma_3$ (σ_1, σ_2, and σ_3 are three principal stresses, major, intermediate, and minor). Considering $\sigma_1 = \sigma_3 + \sigma_d$, $\sigma_2 = \sigma_3$, and $\sigma_3 = \sigma_c$, σ_d representing deviator stress and σ_c denoting confining stress, $\sigma_{sum} = 3\sigma_c + \sigma_d$. Also, τ_{oct} is the octahedral shear stress ($\tau_{oct} = 1/3\sqrt{(\sigma_1 - \sigma_2)^2 + (\sigma_1 - \sigma_3)^2 + (\sigma_2 - \sigma_3)^2}$).

The regression parameters of the clay mixed with different percentages of glass are provided in Table 4 for both models. The coefficient of determination (R^2) values of the specimens are presented as well.

It can be implied from the results of Table 4 that the MEPDG model could model the M_r of the specimens with higher accuracy than the Witczak and Uzan model, as the R^2 values obtained from the MEPDG model vary from 0.91
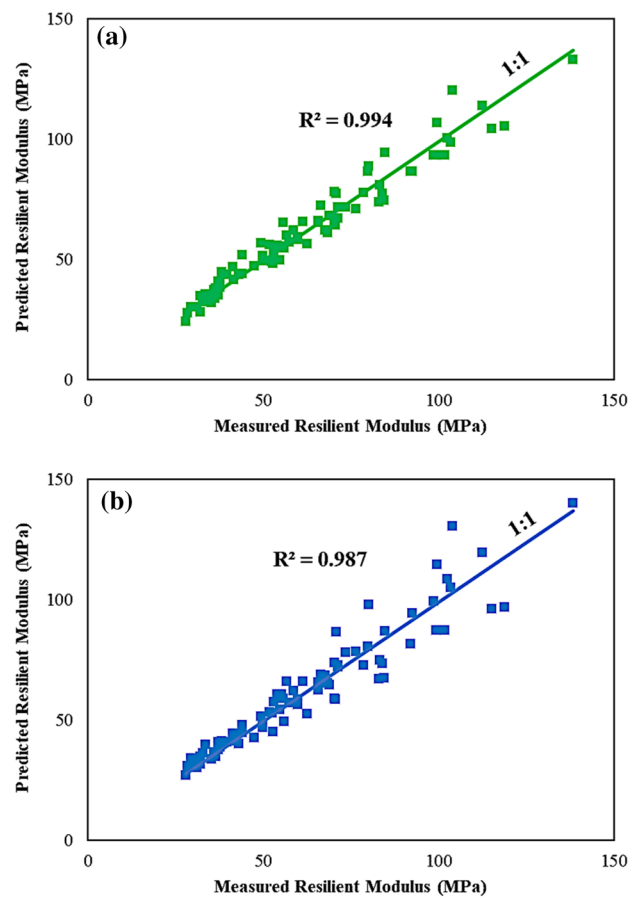

Fig. 12 Relationships between the measured and modelled M_r by **a** MEPDG model and **b** Witczak and Uzan model

to 0.95, whilst the R^2 values of the Witczak and Uzan model are in the range of 0.81–0.97. Another result is that the k_3 constants, which relate to σ_d, of both models had negative values. Thus, it can be inferred that M_r decreases as the σ_d increases. Figure 12 shows that there is a clear linear relationship between the predicted M_r and measured M_r. The both MEPDG model and Witczak and Uzan model provided excellent fits with respective R^2 values of 0.994 and 0.987.

Table 4 The regression parameters of the clay–glass mixtures obtained from the MEPDG model and the Witczak and Uzan model

Specimen	MEPDG model				Witczak and Uzan model			
	k_1	k_2	k_3	r^2	k_1	k_2	k_3	r^2
0% glass	0.84	0.17	−3.81	0.94	0.18	0.19	−0.49	0.97
5% glass	1.06	0.36	−6.88	0.94	0.10	0.37	−0.68	0.89
10% glass	1.22	0.37	−6.75	0.93	0.12	0.37	−0.67	0.85
15% glass	1.52	0.32	−4.91	0.91	0.28	0.32	−0.50	0.81
20% glass	1.31	0.22	−4.30	0.95	0.29	0.22	−0.45	0.86

5 Conclusion

A majority of the previous studies conducted on clay stabilised with glass focus on the introduction of glass in the form of glass residue, glass fine, soda-lime glass powder and powdered glass. The current study evaluated the effect of adding crushed glass (CG) to a low plasticity clay in terms of both mechanical and microstructural properties. The following conclusions could be arrived at through the results of the experimental analysis:

1. Based on the microCT analysis results, the porosity increased with the introduction of CG, which could be elucidated through the reduced packing efficiency of the CG due to its angular particle shape as well as the larger particle size of the CG. The SEM images revealed that the glass has rough surface features, which indicate the possibility of improved frictional resistance.
2. The introduction of CG led to a slight decrease in OMC and an increase in MDD. The decrease in OMC is due to the moisture-insensitive nature (low water absorption) of glass particles.
3. The UCS of the low plasticity clay improved with the addition of CG up until an optimum inclusion of 10% CG. The increase was because of the more efficient interlocking capabilities of the angular CG. Increasing the content of glass beyond 10% increased glass–glass interactions, leading to a decrease in the UCS due to the reduction in the overall cohesion, resulting in reduced frictional resistance.
4. The CBR results showed improvement with the addition of CG up to the maximum inclusion of 20% CG. This being said, the improvement in CBR with each 5% increment of CG was noticed to diminish as the CG content was increased. This could be elucidated in a manner similar to the UCS results so that the inclusion of CG could increase the friction between the clay and glass particles and improve the compact packing of glass with clay particles.
5. The swelling–shrinkage potential of the clay was reduced upon the inclusion of CG, which was expected because of the relative insensitivity to the moisture of CG. Also, the angular nature of the glass could form an effective interlocking mechanism in the clay soil and provide resistance to heaving and shrinkage of the low plasticity clay.
6. The resilient modulus (M_r) values were noted to increase with the addition of CG up to an optimum inclusion of 15%. It is noteworthy that the most remarkable increase was observed as the CG content was increased from 10 to 15%. This being said, the introduction of 20% CG resulted in a decrease in M_r. This could be interpreted through the increased interaction of CG–CG particles with lower cohesion. This resulted in diminishing frictional forces leading to increased settlement, hence decreasing the M_r.
7. The introduction of crushed glass with a lower water absorption capacity, thus having an inferior ability to retain water compared to the clay, led to a decrease in the suction values of the mixes. The higher porosity due to the addition of the glass also contributed to the decrease in the suction values.

From the findings of this study, it was decided that the optimum inclusion which best enhances the overall mechanical and physical properties would be an inclusion of 15% CG, where this inclusion has twofold benefits of improving the low plasticity clay properties as well as providing a sustainable solution to prevent landfilling of waste glass and utilising it for road construction.

Data Availability Statement The datasets generated during and analysed during the current study are available from the corresponding author upon reasonable request.

Declarations

Conflict of Interest The authors report there are no competing interest to declare.

References

1. Wang, G., Li, J., Saberian, M., Rahat, M. H. H., Massarra, C., Buckhalter, C., & Johnson, J. (2022). Use of COVID-19 single-use face masks to improve the rutting resistance of asphalt pavement. *Science of The Total Environment, 826*, 154118. https://doi.org/10.1016/j.scitotenv.2022.154118
2. Soltani, A., Deng, A., Taheri, A., & O'Kelly, B. C. (2019). Engineering reactive clay systems by ground rubber replacement and polyacrylamide treatment. *Polymers, 11*(10), 1675. https://doi.org/10.3390/polym11101675

3. Ural, N. (2018). The importance of clay in geotechnical engineering. *Current Topics in the Utilization of Clay in Industrial and Medical Applications*. https://doi.org/10.5772/intechopen.75817

4. Soltani, A., Taheri, A., Deng, A., & O'kelly, B. C. (2020). Improved geotechnical behavior of an expansive soil amended with tire-derived aggregates having different gradations. *Minerals, 10*(23), 1–20. https://doi.org/10.3390/min10100923

5. Chen, B., Peng, F., Zhang, L., & Sun, D. (2022). Investigation on swelling characteristics of GMZ bentonite with different initial water contents. *Annals of Nuclear Energy, 181*(2023), 109565. https://doi.org/10.1016/j.anucene.2022.109565

6. Zumrawi, M., Abdelmarouf, A., & Gameil, A. (2017). Damages of buildings on expansive soils: Diagnosis and avoidance. *International Journal of Multidisciplinary and Scientific Emerging Research, 6*(2), 108–116.

7. Li, J., Cameron, D. A., & Ren, G. (2014). Case study and back analysis of a residential building damaged by expansive soils. *Computers and Geotechnics, 56*, 89–99. https://doi.org/10.1016/j.compgeo.2013.11.005

8. Ozer, M., Ulusay, R., & Isik, N. S. (2012). Evaluation of damage to light structures erected on a fill material rich in expansive soil. *Bulletin of Engineering Geology and the Environment, 71*(1), 21–36. https://doi.org/10.1007/s10064-011-0395-2

9. Hussein, M. (2021). Effect of sand and sand-lime piles on the behavior of expansive clay soil. *Advances in Civil Engineering, 2021*, 1–11. https://doi.org/10.1155/2021/4927078

10. Schanz, T., & Elsawy, M. B. D. (2015). Swelling characteristics and shear strength of highly expansive clay–lime mixtures: A comparative study. *Arabian Journal of Geosciences, 8*(10), 7919–7927. https://doi.org/10.1007/s12517-014-1703-5

11. Medjnoun, A., & Bahar, R. (2016). Shrinking–swelling of clay under the effect of hydric cycles. *Innovative Infrastructure Solutions, 1*(46), 1–8. https://doi.org/10.1007/s41062-016-0043-6

12. Yang, H. P., & Zheng, J. L. (2006). The new engineering treatment techniques of expansive soils subgrade for Guangxi Nanning-Youyi Guan expressway. *In Unsaturated Soils, 2006*, 439–450.

13. Nelson, J., & Miller, D. J. (1997). *Expansive soils: Problems and practice in foundation and pavement engineering*. Wiley.

14. Maichin, P., Jitsangiam, P., Nongnuang, T., Boonserm, K., Nusit, K., Pra-ai, S., Binaree, T., & Aryupong, C. (2021). Stabilized high clay content lateritic soil using cement-FGD gypsum mixtures for road subbase applications. *Materials, 14*(8), 1858. https://doi.org/10.3390/ma14081858

15. Nitin, T., & Satyam, N. (2019). Experimental study on the influence of polypropylene fiber on the swelling pressure expansion attributes of silica fume stabilized clayey soil. *Geosciences, 9*(9), 377. https://doi.org/10.3390/geosciences9090377

16. Soltani, A., Deng, A., Taheri, A., Mirzababaei, M., & Vanapalli, S. K. (2019). Swell-shrink behavior of rubberized expansive clays during alternate wetting and drying. *Minerals, 9*(4), 1–18. https://doi.org/10.3390/min9040224

17. Dhar, S., & Hussain, M. (2019). The strength behaviour of lime-stabilised plastic fibre-reinforced clayey soil. *Road Materials and Pavement Design, 20*(8), 1757–1778. https://doi.org/10.1080/14680629.2018.1468803

18. Salim, N. M., Al-Soudany, K. Y. H., & Ahmed, A. A. (2018). The impact of using recycled plastic fibres on the geotechnical properties of soft iraqi soils. *IOP Publishing, Bristol, 433*(2018), 1757–8981. https://doi.org/10.1088/1757-899X/433/1/012017

19. Abdulrahman, S. M., Fattah, M. Y., & Ihsan, E. A. (2021). Influence of plastic fiber on the geotechnical properties of gypseous soil. *International Journal of Engineering (Tehran), 34*(2), 367–374. https://doi.org/10.5829/IJE.2021.34.02B.08

20. Kumar, C. R., Gadekari, R. S., Vani, G., & Mini, K. M. (2020). Stabilization of black cotton soil and loam soil using reclaimed asphalt pavement and waste crushed glass. *Materials Today: Proceedings, 24*, 379–387. https://doi.org/10.1016/j.matpr.2020.04.289

21. Malasavage, N. E., Gallagher, P. M., Grubb, D. G., Wartman, J., & Carnivale, M. (2007). Modifying a plastic clay with crushed glass: implications for constructed fills. *Soils and Foundations, 47*(6), 1017–1027. https://doi.org/10.3208/sandf.47.1017

22. Zhao, H., Ge, L., Petry, T. M., & Sun, Y.-Z. (2013). Effects of chemical stabilizers on an expansive clay. *KSCE Journal of Civil Engineering, 18*(4), 1009–1017. https://doi.org/10.1007/s12205-013-1014-5

23. Smaida, A., Mekerta, B., & Gueddouda, M. K. (2021). Physico-mechanical stabilization of a high swelling clay. *Construction and Building Materials, 289*(2021), 123197. https://doi.org/10.1016/j.conbuildmat.2021.123197

24. Alireza, N. S., Negahdar, A., Negahdar, H., & Badakhshan, E. (2021). Stabilised sulfate-rich clay with magnesium oxysulfate cement. *Geomechanics and Geoengineering, 17*(6), 1–11. https://doi.org/10.1080/17486025.2021.1975044

25. Amulya, S., Ravi Shankar, A. U., & Praveen, M. (2020). Stabilisation of lithomargic clay using alkali activated fly ash and ground granulated blast furnace slag. *International Journal of Pavement Engineering, 2*(9), 1114–1121. https://doi.org/10.1080/10298436.2018.1521520

26. Abdullah, H. H., Shahin, M. A., & Walske, M. L. (2020). Review of fly-ash-based geopolymers for soil stabilisation with special reference to clay. *Geosciences, 10*(7), 249. https://doi.org/10.3390/geosciences10070249

27. Karimiazar, J., Teshnizi, S. E., Mirzababaei, M., Mahdad, M., & Arjmandzadeh, R. (2022). California bearing ratio of a reactive clay treated with nano-additives and cement. *Journal of Materials in Civil Engineering, 34*(2), 04021431. https://doi.org/10.1061/(ASCE)MT.1943-5533.0004028

28. Al-Taie, A., Disfani, M., Evans, R., Arulrajah, A., & Horpibulsuk, S. (2019). Volumetric behavior and soil water characteristic curve of untreated and lime-stabilized reactive clay. *International Journal of Geomechanics, 19*(2), 4018192. https://doi.org/10.1061/(ASCE)GM.1943-5622.0001336

29. Ghadir, P., Zamanian, M., Mahbubi-Motlagh, N., Saberian, M., Li, J., & Ranjbar, N. (2021). Shear strength and life cycle assessment of volcanic ash-based geopolymer and cement stabilized soil: A comparative study. *Transportation Geotechnics, 31*, 100639. https://doi.org/10.1016/j.trgeo.2021.100639

30. Nasiri, H., Khayat, N., & Mirzababaei, M. (2021). Simple yet quick stabilization of clay using a waste by-product. *Transportation Geotechnics, 28*(2021), 100531. https://doi.org/10.1016/j.trgeo.2021.100531

31. Saberian, M., Li, J., Perera, S. T. A. M., Zhou, A., Roychand, R., & Ren, G. (2021). Large-scale direct shear testing of waste crushed rock reinforced with waste rubber as pavement base/subbase materials. *Transportation Geotechnics, 28*, 100546. https://doi.org/10.1016/j.trgeo.2021.100546

32. Saberian, M., Li, J., Donnoli, A., Bonderenko, E., Oliva, P., Gill, B., & Siddique, R. (2021). Recycling of spent coffee grounds in construction materials: A review. *Journal of Cleaner Production, 289*, 125837. https://doi.org/10.1016/j.jclepro.2021.125837

33. Islam, S., Islam, J., & Hoque, N. M. R. (2022). Improvement of consolidation properties of clay soil using fine-grained construction and demolition waste. *Heliyon, 8*(10), 11029. https://doi.org/10.1016/j.heliyon.2022.e11029

34. Artuso, F., & Lukiantchuki, J. A. (2019). Evaluation of the self-cemeting effect of construction and demotion waste (CDW) on mechanical performance over time for pavement support layers purpose. *Ambiente Construído, 19*, 59–77. https://doi.org/10.1590/s1678-86212019000200308

35. Arulrajah, A., Mohammadinia, A., Maghool, F., & Horpibulsuk, S. (2019). Tyre derived aggregates and waste rock blends: Resilient moduli characteristics. *Construction and Building Materials, 201*, 207–217. https://doi.org/10.1016/j.conbuildmat.2018.12.189

36. Arulrajah, A., Mohammadinia, A., Maghool, F., & Horpibulsuk, S. (2019). Tire derived aggregates as a supplementary material with recycled demolition concrete for pavement applications. *Journal of Cleaner Production, 230*, 129–136. https://doi.org/10.1016/j.jclepro.2019.05.084

37. Kazmi, D., Serati, M., Williams, D. J., Qasim, S., & Cheng, Y. P. (2021). The potential use of crushed waste glass as a sustainable alternative to natural and manufactured sand in geotechnical applications. *Journal of Cleaner Production, 284*, 124762. https://doi.org/10.1016/j.jclepro.2020.124762

38. Disfani, M. M., Tsang, H. H., Arulrajah, A., & Yaghoubi, E. (2017). Shear and compression characteristics of recycled glass-tire mixtures. *Journal of Materials in Civil Engineering, 29*(6), 06017003. https://doi.org/10.1061/(ASCE)MT.1943-5533.0001857

39. Ferdous, W., Manalo, A., Siddique, R., Mendis, P., Zhuge, Y., Wong, H. S., Lokuge, W., Aravinthan, T., & Schubel, P. (2021). Recycling of landfill wastes (tyres, plastics and glass) in construction—A review on global waste generation, performance, application and future opportunities. *Resources, Conservation and Recycling, 173*(2021), 105745. https://doi.org/10.1016/j.resconrec.2021.105745

40. Rivera, J. F., Cuarán-Cuarán, Z. I., Vanegas-Bonilla, N., & Mejía de Gutiérrez, R. (2018). Novel use of waste glass powder: Production of geopolymeric tiles. *Advanced Powder Technology, 29*(12), 3448–3454. https://doi.org/10.1016/j.apt.2018.09.023

41. Escalante-Garcia, J. I. (2015). Overview of potential of urban waste glass as a cementitious material in alternative chemically activated binders. *Journal of Chinese Ceramic Society, 43*(10), 1441–1448. https://doi.org/10.14062/j.issn.0454-5648.2015.10.14

42. Robert, D., Baez, E., & Setunge, S. (2021). A new technology of transforming recycled glass waste to construction components. *Construction and Building Materials, 313*(2021), 125539. https://doi.org/10.1016/j.conbuildmat.2021.125539

43. Kazmi, D., Williams, D. J., & Serati, M. (2019). Waste glass in civil engineering applications—A review. *International Journal of Applied Ceramic Technology, 17*(2), 529–554. https://doi.org/10.1111/ijac.13434

44. Flood, M., Fennessy, L., Lockrey, S, Avendano Franco, A, Glover, J, Kandare, E., & Bhat, T. (2020). Glass Fines: Final Report, S Victoria. Retrieved January 12, 2022, from https://assets.sustainability.vic.gov.au/susvic/Report-Waste-Glass-Fines-RMIT.pdf

45. Van Yken, J., Boxall, N. J., Cheng, K. Y., Nikoloski, A. N., Moheimani, N. R., & Kaksonen, A. H. (2021). E-waste recycling and resource recovery: A review on technologies, barriers and enablers with a focus on oceania. *Metals, 11*(8), 1–40. https://doi.org/10.3390/met11081313

46. Singh, N., Li, J., & Zeng, X. (2016). Solutions and challenges in recycling waste cathode-ray tubes. *Journal of Cleaner Production, 133*(2016), 188–200. https://doi.org/10.1016/j.jclepro.2016.04.132

47. Junak, J. (2015). Utilization of crushed glass waste in concrete samples prepared with coal fly ash. *Solid State Phenomena, 244*, 102–107. https://doi.org/10.4028/www.scientific.net/SSP.244.102

48. Henke, T., Speranza, M. G., & Wäscher, G. (2015). The multi-compartment vehicle routing problem with flexible compartment sizes. *European Journal of Operational Research, 246*(3), 730–743. https://doi.org/10.1016/j.ejor.2015.05.020

49. Luhar, S., Cheng, T.-W., Nicolaides, D., Luhar, I., Panias, D., & Sakkas, K. (2019). Valorisation of glass waste for development of geopolymer composites—Mechanical properties and rheological characteristics: A review. *Construction and Building Materials, 220*(2019), 547–564. https://doi.org/10.1016/j.conbuildmat.2019.06.041

50. Más-López, M. I., Garcia del Toro, E. M., Patiño, A. L., & García, L. J. M. (2020). Eco-friendly pavements manufactured with glass waste: Physical and mechanical characterization and its applicability in soil stabilization. *Materials, 13*(17), 1–13. https://doi.org/10.3390/ma13173727

51. Harrison, E., Berenjian, A., & Seifan, M. (2020). Recycling of waste glass as aggregate in cement-based materials. *Environmental Science and Ecotechnology, 4*(2020), 100064. https://doi.org/10.1016/j.ese.2020.100064

52. Saberian, M., Li, J., Boroujeni, M., Law, D., & Li, C.-Q. (2020). Application of demolition wastes mixed with crushed glass and crumb rubber in pavement base/subbase. *Resources, Conservation and Recycling, 156*, 104722. https://doi.org/10.1016/j.resconrec.2020.104722

53. Monich, P. R., Romero, A. R., Höllen, D., & Bernardo, E. (2018). Porous glass-ceramics from alkali activation and sinter-crystallization of mixtures of waste glass and residues from plasma processing of municipal solid waste. *Journal of Cleaner Production, 188*(2018), 871–878. https://doi.org/10.1016/j.jclepro.2018.03.167

54. Rincón, A., Marangoni, M., Cetin, S., & Bernardo, E. (2016). Recycling of inorganic waste in monolithic and cellular glass-based materials for structural and functional applications. *Journal of Chemical Technology & Biotechnology, 91*(7), 1946–1961. https://doi.org/10.1002/jctb.4982

55. Drăgoescu, M. F., & Păunescu, L. (2020). Porous material from recycled glass waste as an alternative to existing building materials. *Constructii, 21*(2), 48–56.

56. Belebchouche, C., Moussaceb, K., Bensebti, S.-E., Aït-Mokhtar, A., Hammoudi, A., & Czarnecki, S. (2021). Mechanical and microstructural properties of ordinary concrete with high additions of crushed glass. *Materials, 14*(1872), 1–16. https://doi.org/10.3390/ma14081872

57. Kioko, P. C. K. (2021). An assessment into the use of crushed glass as partial replacement for fine aggregates. *International Journal of Engineering Research & Technology (IJERT), 10*(2), 364–398. https://doi.org/10.17577/IJERTV10IS020176

58. Wartman, J., Grubb, D. G., & Nasim, A. S. M. (2004). Select engineering characteristics of crushed glass. *Journal of Materials in Civil Engineering, 16*(6), 526–539. https://doi.org/10.1061/(ASCE)0899-1561(2004)16:6(526)

59. Liu, Y., Shi, C., Zhang, Z., & Li, N. (2019). An overview on the reuse of waste glasses in alkali-activated materials. *Resources, Conservation and Recycling, 144*(2019), 297–309. https://doi.org/10.1016/j.resconrec.2019.02.007

60. Gorospe, K., Booya, E., Ghaednia, H., & Das, S. (2019). Strength, durability, and thermal properties of glass aggregate mortars. *Journal of Materials in Civil Engineering, 31*(10), 04019231. https://doi.org/10.1061/(ASCE)MT.1943-5533.0002884

61. Chung, S.-Y., Abd Elrahman, M., Sikora, P., Rucinska, T., Horszczaruk, E., & Stephan, D. (2017). Evaluation of the effects of crushed and expanded waste glass aggregates on the material properties of lightweight concrete using image-based approaches. *Materials (Basel, Switzerland), 10*(12), 1354. https://doi.org/10.3390/ma10121354

62. Salamtpoor, S., & Salamatpoor, S. (2017). Evaluation of adding crushed glass to different combinations of cement-stabilized sand. *International Journal of Geo-Engineering, 8*(8), 1–12. https://doi.org/10.1186/s40703-017-0044-0

63. Singh, S., Agareal, V. C., & Srivastava, V. (2015). Glass waste in concrete: Effect on workability and compressive strength. *International Journal of Innovative Research in Science, Engineering and Technology, 4*(9), 8142–8150. https://doi.org/10.15680/IJIRSET.2015.0409018

64. Kassed, G., & Ali, S. (2021). Reuse of glass waste as a partial replacement to fine aggregates in concrete. *Journal of Engineering, 27*(8), 43–58. https://doi.org/10.31026/j.eng.2021.08.04

65. So, S. T. C., Lee, R. M. K., Hui, T., & Shiu, Y. K. (2015). Study of using recycled glass cullet as an engineering fill in reclaimation and earthworks in Hong Kong. *Japanese Geotechnical Society Special Publication, 2*(54), 1864–1879. https://doi.org/10.3208/jgssp.HKG-14

66. Disfani, M. M., Tsang, H.-H., Arulrajah, A., & Yaghoubi, E. (2017). Shear and compression characteristics of recycle glass-tire mixtures. *Journal of Materials in Civil Engineering, 29*(6), 06017003. https://doi.org/10.1061/(ASCE)MT.1943-5533.0001857

67. Cozzarini, L., Marsich, L., Ferluga, A., & Schmid, C. (2020). Life cycle analysis of a novel thermal insulator obtained from recycled glass waste. *Developments in the Built Environment, 3*(2020), 100014. https://doi.org/10.1016/j.dibe.2020.100014

68. Saltan, M., Öksüz, B., & Uz, V. E. (2015). Use of glass waste as mineral filler in hot mix asphalt. *Science and Engineering of Composite Materials, 22*(3), 271–277. https://doi.org/10.1515/secm-2013-0135

69. Bagheri, A., & Moukannaa, S. (2021). A new approach to the reuse of waste glass in the production of alkali-activated materials. *Cleaner Engineering and Technology, 4*, 100212. https://doi.org/10.1016/j.clet.2021.100212

70. Oliveira, R., de Brito, J., & Veiga, R. (2015). Reduction of the cement content in rendering mortars with fine glass aggregates. *Journal of Cleaner Production, 95*, 75–88. https://doi.org/10.1016/j.jclepro.2015.02.049

71. Majdinasab, A., & Yuan, Q. (2019). Post-consumer cullet and potential engineering applications in North America. *Resources, Conservation and Recycling, 147*(2019), 1–9. https://doi.org/10.1016/j.resconrec.2019.04.009

72. Perera, S. T. A. M., Zhu, J., Saberian, M., Liu, M., Cameron, D., Maqsood, T., & Li, J. (2021). Application of glass in subsurface pavement layers: A comprehensive review. *Sustainability*. https://doi.org/10.3390/su132111825

73. Saberian, M., Li, J., & Setunge, S. (2019). Evaluation of permanent deformation of a new pavement base and subbase containing unbound granular materials, crumb rubber and crushed glass. *Journal of Cleaner Production, 230*, 38–45. https://doi.org/10.1016/j.jclepro.2019.05.100

74. Yaghoubi, E., Al-Taie, A., Disfani, M., & Fragomeni, S. (2021). Recycled aggregate mixtures for backfilling sewer trenches in nontrafficable areas. *International Journal of Geoemchanics, 22*(3), 04021308. https://doi.org/10.1061/(ASCE)GM.1943-5622.0002297

75. Fauzi, A., Djauhari, Z., & Fauzi, U. J. (2016). Soil engineering properties improvement by utilization of cut waste plastic and crushed waste glass as additive. *International Journal of Engineering and Technology, 8*(1), 15–18. https://doi.org/10.7763/IJET.2016.V8.851

76. Do, A., Sule, E., & Bakam, V. A. (2021). Performance evaluation of crushed glass in stabilizing lateritic soil for road pavement layers. *Saudi Journal of Engineering and Technology, 6*(4), 77–83. https://doi.org/10.36348/sjet.2021.v06i04.006

77. Eberemu, A. O., Edeh, J. E., & Gbolokun, A. O. (2013). The geotechnical properties of lateritic soil treated with crushed glass cullet. *Advanced Materials Research, 824*(2013), 21–28. https://doi.org/10.4028/www.scientific.net/AMR.824.21

78. Babatunde, O. A., Sani, E. J., & Sambo, H. (2019). Black cotton soil stabilization using glass powder. *RIET-IJSET International Journal of Science Engineering and Technology, 8*(5), 5208–5214. https://doi.org/10.15680/IJIRSET.2019.0805053

79. Canakci, H., Al-Kaki, A., & Celik, F. (2016). Stabilization of clay with waste soda lime glass powder. *Procedia Engineering, 161*(2016), 600–605. https://doi.org/10.1016/j.proeng.2016.08.705

80. Abbey, S. J., Eyo, E. U., Oti, J., Amakye, S. Y., & Ngambi, S. (2020). Mechanical properties and microstructure of fibre-reinforced clay blended with by-product cementitious materials. *Geosciences, 10*(241), 1–18. https://doi.org/10.3390/geosciences10060241

81. Yogeshraj, U. C., Thejas H. K., & Nanjunda, K. N. (2020). Effect of glass and coir fiber on geotechnical properties of clayey soil. *International Journal of Advanced Science and Technology, 29*(3), 5212–5218. http://sersc.org/journals/index.php/IJAST/article/view/6027

82. Rabab'ah, S., Al Hattamleh, O., Aldeeky, H., & Abu Alfoul, B. (2021). Effect of glass fiber on the properties of expansive soil and its utilization as subgrade reinforcement in pavement applications. *Case Studies in Construction Materials, 14*(2021), e00485. https://doi.org/10.1016/j.cscm.2020.e00485

83. Whyndham City Council. (2021). Whyndham City Council Plan 2021–25. https://www.wyndham.vic.gov.au/about-council/your-council/plans-policies-strategies/wyndham-city-council-plan-2021-25. Viewed 18/02/2022

84. Saberian, M., Perera, S. T. A. M., Li, J., Zhu, J., & Wang, G. (2021). Effect of crushed glass on the shear behavior of recycled unbound granular aggregates incorporating crumb rubber. *International Journal of Pavement Research & Technology, 15*, 1079–1092. https://doi.org/10.1007/s42947-021-00073-7

85. AS 1289.3.6.1. (2009). *Methods of testing soils for engineering purposes-Soil classification tests—Determination of the particle size distribution of a soil—Standard method of analysis by sieving*. Australian Standard AS 1289.3.6.1, Australian Standard.

86. AS 1289.3.6.3. (2020). *Methods of testing soils for engineering purposes, Part 3.6.3: Soil classification tests—Determination of the particle size distribution of a soil—Standard method of fine analysis using an hydrometer*. Australian Standard 1289.3.6.3, Australian Standard.

87. Day, N. (2022). *Crystallography open database*. Department of Chemistry, Unversity of Cambridge. 2022.

88. Lotero, A., Consoli, N. C., Moncaleano, C. J., Neto, A. T., & Koester, E. (2021). Mechanical properties of alkali-activated ground waste glass–carbide lime blends for geotechnical uses. *Journal of Materials in Civil Engineering, 33*(10), 04021284. https://doi.org/10.1061/(ASCE)MT.1943-5533.0003918

89. Irshidat, M. R., Al-Saleh, M. H., & Sanad, S. (2015). Effect of nanoclay on the expansive potential of cement mortar due to alkali-silica reaction. *ACI Materials Journal, 112*(6), 801–808. https://doi.org/10.14359/51687856

90. Demir, I. (2009). Reuse of waste glass in building brick production. *Waste Management & Research, 27*(6), 572–577. https://doi.org/10.1177/0734242X08096528

91. ASTM D422. (2007). *Standard test method for particle size analysis of soils*. ASTM.

92. ASTM D4318. (2000). *Standard test method for liquid limit, plastic limit, and plasticity index of soils*. ASTM.

93. AS 1289.7.1.1. (2003). *Method of testing soils for engineering purposes/soil reactivity tests-Determination of the shrinkage index of a soil-Shrink-swell index*. Australian standard 1289.7.1.1, Australian Standard (pp. 1–9).

94. ASTM D2487. (2011). *Standard practice for classification of soils for engineering purposes (unified soil classification system*. ASTM.

95. ASTM D854. (2010). *Standard test methods for specific gravity of soil solids by water pycnometer*. ASTM.

96. AS 1289.3.4.1. (2008). *Methods of testing soils for engineering purposes Soil classification tests - Determination of the linear shrinkage of a soil—Standard method*. Australian Standard 1289.3.4.1, Australian Standard (pp. 1–13).

97. AS 1289.5.1.1. (2017). *Methods of testing soils for engineering purposes Soil compaction and density tests—Determination of the dry density/moisture content relation of a soil using standard compactive effort*. Australian Standard 1289.5.1.1, Australian Standard (pp. 1–13).

98. AS 1289.6.1.1. (2014). *Soil strength and consolidation tests—Determination of the California bearing ratio of a soil-standard laboratory method for a remoulded specimen*. Australian Standard 1289.6.1.1, Australian Standard (pp. 1–25).

99. AS 5101.4. (2008). *Unconfined compressive strength of compacted materials*. Australian Standard 5101.4, Australian Standard (pp. 1–13).

100. Raja, M. N. A., Shukla, S. K., & Khan, M. U. A. (2021). An intelligent approach for predicting the strength of geosynthetic-reinforced subgrade soil. *International Journal of Pavement Engineering, 23*(10), 3505–3521. https://doi.org/10.1080/10298436.2021.1904237

101. Xiao, Y., Zheng, K., Chen, L., & Mao, J. (2018). Shakedown analysis of cyclic plastic deformation characteristics of unbound granular materials under moving wheel loads. *Construction and Building Materials, 167*(2018), 457–472. https://doi.org/10.1016/j.conbuildmat.2018.02.064

102. Protocol P46. (1996). *Long-Term Pavement Performance Protocol P46 (1996). Resilient modulus of unbound granular base/subbase materials and subgrade soils*. U.S. Department of Transportation, Federal Highway Administration.

103. Suits, L., Sheahan, T. C., Fityus, S. G., Cameron, D., & Walsh, P. F. (2005). The shrink swell test. *Geotechnical Testing Journal, 28*(1), 1–10. https://doi.org/10.1520/GTJ12327

104. Li, J., Zou, J., Bayetto, P., & Barker, N. (2016). Shrink-swell index database for Melbourne. *Australian Geomechanics Journal, 51*, 61–76.

105. Yamusa, Y. B., Hezmi, M. A., Ahmad, K., & Kassim, K. A. (2018). Using soil water characteristic curve in computing unsaturated hydraulic conductivity of compcted tropical soil. *APRN Journal of Engineering and Applied Sciences, 13*(17), 4765–4770.

106. Silva, M.L.-N., Libardi, P. L., & Gimenes, F. H. S. (2018). Soil water retention curve as affected by sample height. *Revista Brasileira de Ciencia do Solo, 42*(2018), 1–13. https://doi.org/10.1590/18069657rbcs20180058

107. ASTM D6836. (2016). *Test methods for determination of the soil water characteristic curve for de- sorption using a hanging column, pressure extractor, chilled mirror hygrometer, and/or centrifuge*. ASTM.

108. Gurjar, J., Agarwal, P. K., & Sharma, M. J. (2013). A framework for quantification of effect of drainage quality on structural and functional performance of pavement. *International Journal of Engineering Research, 2*, 262–264.

109. Dungca, J. R., Lao, W. D. T., Lim, M., Lu, W. D., & Redelicia, J. C. P. (2019). Radial flow permeameter: A proposed apparatus to measure horizontal hydraulic gradient of fly-ash based geopolymer-soil mix. *International Journal of GEOMATE, 6*(58), 218–223. https://doi.org/10.21660/2019.58.4524

110. Rokade, S., Agarwal, P. K., & Srivastava, R. (2012). Drainage and flexible pavement performance. *Internation al journal of Engineering Science and Technology (IJEST), 4*(4). 1308–1311. http://www.ijest.info/docs/IJEST12-04-04-072.pdf

111. Shaikh, S. G., & Wadekar, A. P. (2021). Systematic evaluation and analysis of bituminous road pavement failure. *Journal of Physics: Conference Series.* https://doi.org/10.1088/1742-6596/1964/7/072016

112. Saeed, F., Rahman, M., & Chamberlain, D. (2018). A novel laboratory test method to measure dynamic water pressure underneath a cracked concrete pavement. In *2018 LJMU annual international conference on: Apshalt, pavement engineering and infrastructure*. http://bura.brunel.ac.uk/handle/2438/16035

113. Vervoot, R. W., & Cattle, S. R. (2003). Linking hydraulic conductivity and tortuosity parameters to pore space geometry and pore-size distribution. *Journal of Hydrology, 272*(2003), 36–49. https://doi.org/10.1016/S0022-1694(02)00253-6

114. Wang, S., Zhu, W., Fei, K., Xu, C., & Zhang, N. (2018). Study on non-darcian flow sand-clay mixtures. *Applied Clay Science, 151*(2018), 102–108. https://doi.org/10.1016/j.clay.2017.10.028

115. Al-Kaissi, Z. A., & Mashkoor, O. G. (2016). Durability of porous asphalt pavement. *Journal of Engineering and Sustainable Development, 20*(4), 53–70.

116. Khan, M., Tufail, M., & Mateeullah, M. (2018). Effects of waste glass powder on the geotechnical properties of loose subsoils. *Civil Engineering Journal, 4*(9), 2044–2051. https://doi.org/10.28991/cej-03091137

117. Bilgen, G. (2020). Utilization of powdered glass as an additive in clayey soils. *Geotechnical and Geological Engineering, 38*(3), 3163–3173. https://doi.org/10.1007/s10706-020-01215-7

118. Saberian, M., Li, J., & Cameron, D. (2019). Effect of crushed glass on behavior of crushed recycled pavement materials together with crumb rubber for making a clean green base and subbase. *Journal of Materials in Civil Engineering, 31*(7), 4019108. https://doi.org/10.1061/(ASCE)MT.1943-5533.0002765

119. Blayi, R. A., Sherwani, A. F. H., Ibrahim, H. H., Faraj, R. H., & Daraei, A. (2020). Strength improvement of expansive soil by utilizing waste glass powder. *Case Studies in Construction Materials, 13*(2020), e00427. https://doi.org/10.1016/j.cscm.2020.e00427

120. Javed, S. A., & Chakraborty, S. (2020). Effects of waste glass powder on subgrade soil improvement. *World Scientific News, 144*(2020), 30–42.

121. Mosa, A. M., Al-Dahlaki, M. H., & Salem, L. A. (2021). Modification of roadbed soil by crushed glass wastes. *Periodicals of Engineering and Natural Sciences (PEN), 9*(2), 1038–1045. https://doi.org/10.21533/pen.v9i2.2029

122. Ikara, I., Kundiri, A., & Mohammed, A. (2015). Effects of waste glass (WG) on the strength characteristics of cement stabilized expansive soil. *American Journal of Engineering Research (AJER), 4*(11), 33–41.

123. Joseph, J. K., Benny, J. R., Sebastian, J. M., & Thomas, M. (2017). Effect of glass powder on engineering properties of clayey soil. *International Journal of Engineering Research and Technology, 6*(5), 228–231.

124. Li, D., & Selig, E. T. (1994). Resilient modulus for fine-grained subgrade soils. *Journal of Geotechnical Engineering, 120*(6), 939–957. https://doi.org/10.1061/(ASCE)0733-9410(1994)120:6(939)

125. Yaghoubi, E., Yaghoubi, M., Guerrieri, M., & Sudarsanan, N. (2021). Improving expansive clay subgrades using recycled glass: Resilient modulus characteristics and pavement performance. *Construction and Building Materials, 302*(2021), 124384. https://doi.org/10.1016/j.conbuildmat.2021.124384

126. Ebrahimi-Birang, N., & Fredlund, D. (2016). Assessment of the WP4-T device for measuring total suction. *ASTM International*. https://doi.org/10.1520/GTJ20150118

127. Esmaili, D., & Hatami, K. (2017). Comparative study of measured suction in fine-grained soil using different in-situ and laboratory techniques. *International Journal of Geosynthetics*

and Ground Engineering, 3(27), 1–9. https://doi.org/10.1007/s40891-017-0104-8

128. Fredlund, D. G., & Xing, A. (1994). Equations for the soil–water characteristic curve. *Canadian Geotechnical Journal, 31*, 521–532. https://doi.org/10.1139/t94-061

129. Dafalla, M. A., Al-Mahbashi, A. M., Almajed, A., & Al-Shamrani, M. (2020). Predicting soil-water characteristic curves of clayey sand soils using area computation. *Mathematical Problems in Engineering, 2020*, 1–9. https://doi.org/10.1155/2020/4548912

130. Syarifudin, A., & Satyanaga, A. (2021). Variability of bimodal soil-water characteristic curves under different confining pressures. *Applied and Environmental Soil Science, 2021*, 1–9. https://doi.org/10.1155/2021/5569491

131. Zhou, A.-N., Sheng, D., & Carter, J. P. (2012). Modelling of the effect of initial density on soil water characteristic curves. *Géotechnique, 62*(8), 669–680. https://doi.org/10.1680/geot.10.P.120

132. Ibrahim, H. H., Mawlood, Y. I., & Alshkane, Y. M. (2021). Using waste glass powder for stabilizing high-plasticity clay in Erbil city-Iraq. *International Journal of Geotechnical Engineering, 15*(4), 496–503. https://doi.org/10.1080/19386362.2019.1647644

133. Yaghoubi, E., Sudarsanan, N., & Arulrajah, A. (2021). Stress-strain response analysis of demolition wastes as aggregate base course of pavements. *Transportation Geotechnics, 30*(2021), 100599. https://doi.org/10.1016/j.trgeo.2021.100599

134. Zamin, B., Nasir, D., Farooq, A., & Jehan, B. (2021). Effect of waste glass powder on the swelling and strength characteristic of karak expansive clay. *Sir Syed Research Journal of Engineering & Technology, 11*(2), 1–8. https://doi.org/10.33317/ssurj.362

135. AASHTO. (2008). *Mechanicstic-empirical pavement design guide. A manual of practice.* AASHTO MEPDG-1.

136. Witczak, M. W., & Uzan, J. (1988). *The universal airport pavement design system: Report I of V: Granular material characterization*. University of Maryland.

These include recycled concrete aggregate, crushed waste rock and crumb rubber from waste tyres, focusing on a circular economy and sustainable approach within the civil engineering research arena. In addition, Dr Perera has sound knowledge on construction polymers and chemical additives in engineering materials, given his ongoing employment in a renowned polymer manufacturing company over the past years.

Mohammad Saberian is a professional and experienced civil engineer, having a PhD in Civil Engineering—Geotechnical Engineering from RMIT University. Dr Saberian has outstanding knowledge and research background in the fields of geotechnics, pavements, concrete and infrastructures, artificial neural network, circular economy and sustainability, waste management, applications of waste materials in civil engineering, soil stabilizations, foundations, earthworks, slope stability, dry mix, cementitious compounds, construction materials, binders, and the chemistry of materials.
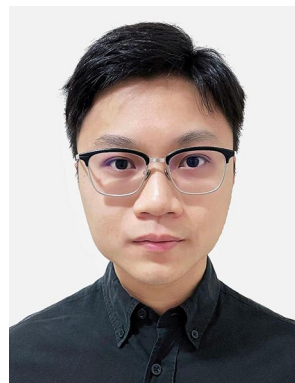
Jiasheng Zhu is a PhD candidate in the Discipline of Civil & Infrastructure Engineering at RMIT University. His major research interests are stabilization and reinforcement of expansive clay soils, pavement structural improvements including base, subbase and subgrade layers, and green & sustainable asphalt. He has published 5 Scopus-indexed journal papers so far.

Salpadoru Tholkamudalige Anupiya. M. Perera is an experienced civil engineer with a PhD in Civil Engineering (Geotechnical Engineering) from RMIT University, Melbourne. Dr Perera has a research background in the field of stabilizing expansive soils for pavement subgrade utilizing non-conventional aggregates such as crushed waste glass and polymer additives. He has further experience in experimental undertakings relating to the utilization of waste materials in engineering applications.

Rajeev Roychand is a Research Fellow at RMIT University with more than 18 years of experience in material research and structure design. He has an extensive track record in material research with high-impact research publications, some of which have been extensively covered by the international media. He has received $862,786 of research funding to date. He has recently been awarded RMIT Award for Impact and Collaboration – Team Award.

Jie Li is a Professor in Geotechnical Engineering at RMIT University with more than 25 years of professional experience as a consulting engineer, laboratory manager, researcher and lecturer. He is a recognized expert in unsaturated soil, pavement geotechnics, recycled materials and ground improvement. His research has been funded by ARC Discovery and Linkage grants. He has a long history of applied research and published over 130 Scopus-indexed journal papers, with over 60 publications in the last 3 years.

Morteza Tahmasebi Yamchelou received his Bachelor's degree in Civil Engineering in 2014 and his Master's degree in Earthquake Engineering in 2016. During his PhD at the Royal Melbourne Institute of Technology between 2018 and 2021, he investigated the development of clay-based geopolymers. After graduation, he started a career as a structural Engineer at the Department of Transport of Victoria, which still continues.

Gang Ren received his PhD degree in Rock Mechanics from the University of Nottingham, UK, in 1988. He is currently an associate in Geotechnical engineering professor at RMIT University. His research interests include slope stability analysis, soil nailing and ground ancho, ground movements and their effects on structures, in situ soil testing, excavation and lateral support design, rock mechanics, surface subsidence analysis and prediction.